1   Totten Ice Shelf history over the past century interpreted from satellite imagery

3   Bertie W.J. Miles[1], Tian Li[2], Robert G. Bingham[1]

4   [1]School of GeoSciences, Edinburgh University, Edinburgh, UK

5   [2]Bristol Glaciology Centre, School of Geographical Sciences, University of Bristol, Bristol,

6   UK

8   *Correspondence to Bertie.Miles@ed.ac.uk

10   **Abstract:** Totten Glacier is currently the largest source of mass loss in the East Antarctic Ice

11   Sheet ~~and it is projected to be a large source of sea-level rise over the coming century~~. The

12   glacier has been losing mass for decades and inland thinning was detected in the earliest

13   satellite-altimetry observations in the early 1990s, but ~~when the glacier first started~~for how

14   long the glacier has been losing mass remains unknown. We calculate decadal ice-speed

15   anomalies to confirm that Totten Glacier has not undergone sustained acceleration since at least

16   1973. Together with observations of grounding-line retreat from 1973-1989, we confirm that

17   the glacier was ~~already out of balance~~losing mass in the 1970s. Surface undulations form on

18   ~~the~~ Totten Ice Shelf ~~adjacent to an ice rumple~~close to a bathymetric high point near the

19   grounding line in response to time-varying melt rates and are preserved downstream for several

20   decades. ~~From utilizing the full suite of Landsat imagery~~Using the full Landsat archive, we

21   produce a century-long record of surface-undulation formation that we interpret as a qualitative

22   record of basal-melt-rate variability. An anomalous ~20-year absence of undulations associated

23   with the mid-20th century manifests a period when ice passing close to a bathymetric high point

24   near the grounding line ~~over the ice rumple~~ was pervasively thinner, and may represent an

25   anomalous~~anonymously~~ warm period that triggered the onset of modern-day mass loss at

26   Totten Glacier. We also observe the collapse of a nearby small ice shelf between 1963 and

27   1973, that is consistent with a regionalised mid-20th century warm period. ~~Our~~ Our results highlight

28   that the currently available ~30-year ~~satellite~~ satellite-altimetry records are not long enough to

29   capture the full scale of decadal variability in basal-melt rates and mass-loss patterns.

30   **1. Introduction**

31   Aurora Subglacial Basin (ASB), located in Wilkes Land, East Antarctica, is drained by five

32   major outlet glaciers: Holmes, Moscow University, Totten, Vanderford and Denman glaciers

33   (Fig. 1). Oceanographic observations have confirmed the presence of warm modified

34   Circumpolar Deep Water (mCDW) on the continental shelf adjacent to each of these outlet

35   glaciers (Ribeiro et al., 2021; Rintoul et al., 2016; Silvano et al., 2017; van Wijk et al., 2022).

36   This is accompanied by ongoing grounding-line retreat (Brancato et al., 2020; Li et al., 2023b;

37   Li et al., 2015; Picton et al., 2023), detachment of ~~the~~ ice shel~~ves~~f from pinning points (Miles

38   and Bingham, 2024)~~,~~ and ice-front retreat (Baumhoer et al., 2021; Miles et al., 2016) identified

39   from satellite observations. The rate of mass loss of ASB between 2003 and 2019 is estimated

40   at -20 Gt yr^{-1} (Smith et al., 2020), meaning that mass loss from ASB has accounted for just

under 2% of global sea-level rise over this period. Pal~~a~~eo-reconstructions from a variety of geological evidence show that ASB may have made multi-metre contributions to global sea-level rise during the warm periods of the mid-Pliocene (Aitken et al., 2016; Cook et al., 2014) when CO_2 concentrations were comparable to the present day (Martínez-Botí et al., 2015). Therefore, indications from the past and observations of current mass loss suggest that ASB has the potential to make globally significant contributions to sea-level rise in the coming decades to centuries (Stokes et al., 2022).

Ice discharge from Totten Glacier (Fig. 1) is estimated to be between 65 and 85 Gt yr^{-1} (Davison et al., 202~~3~~5; Rignot et al., 2019), and ~~it~~ is the single largest source of mass loss from both ASB and the entire East Antarctic Ice Sheet (Mohajerani et al., 2018; Nilsson et al., 2022; Rignot et al., 2019; Schröder et al., 2019; Smith et al., 2020). Inland thinning of ~~Totten Glacier~~grounded ice was detected in the early 1990s (Nilsson et al., 2022; Schröder et al., 2019), hinting that the catchment may have been losing mass decades before the earliest satellite-altimetry observations, but the onset date of this current bout of mass loss is unclear. Recent evidence shows that enhanced intrusion of mCDW is the most likely forcing of the mass loss at Totten Glacier. The warm ocean water can flow over the continental shelf (Rintoul et al., 2016) and travel beneath Totten Ice Shelf towards the grounding line via a network of deep bathymetric troughs (Hirano et al., 2023), leading to significant basal melting. However, whether and how this oceanic forcing has varied over time is unknown, ~~and contributing~~leading to large uncertainties in quantifying sea-level rise contributions from Totten Glacier over the coming century and beyond under a variety of different ~~climate~~ climate-warming scenarios (Jordan et al., 2023; McCormack et al., 2021; Pelle et al., 2021).

Outlet glaciers lose mass through a flux imbalance, whereby ice loss from ice discharge outweighs mass gain from surface mass balance processes. ~~can lose mass through a dynamical acceleration in ice discharge into the ocean, a reduction in snowfall, or a combination of both. Unequivocal evidence shows that major outlet glaciers in West Antarctica that have consistently been losing mass since the onset of satellite observations are doing so in response to a dynamic-thinning-induced acceleration in ice-flow speed, forced initially by thinning to the impounding ice shelves (Kim et al., 2024). However~~At Totten Glacier, despite its significant mass loss across the satellite era, existing studies show no clear widespread acceleration in ice-flow speed across the Totten system (Li et al., 2023a; Li et al., 2015; Rignot et al., 2019; Roberts et al., 2018)~~, and ice core records from the nearby Law Ice Dome (Fig. 1a) show no multi-decadal trends in snowfall.~~. Therefore, the apparent absence ~~of a clear shelf-wide acceleration at Totten could be explained b~~of increased ice discharge over the satellite era could be explained by two possibilities: 1) Sparse and lower quality satellite images pre-2000s are not of sufficient quality to capture ice-flow acceleration ~~of the Totten system~~the glacier or ice shelf, or 2) ~~Totten accelerated before the~~There was already a flux imbalance at the onset of the satellite era, meaning the Totten catchment was already ~~out of balance~~losing mass at the onset of satellite observations.

Here, we analyse ARGON and Landsat optical imagery to investigate the behaviour of the Totten glacier and ice-shelf system over the past century. We calculate decadal ice-speed anomalies and grounding-line migration back to 1973. We also produce a century-long record of surface-undulation formation that can be taken as a qualitative record of basal-melt anomalies. We use all three datasets to determine a broad mass-loss history of ~~the likely timing for the onset of mass loss at~~ Totten Glacier.

86

87

88
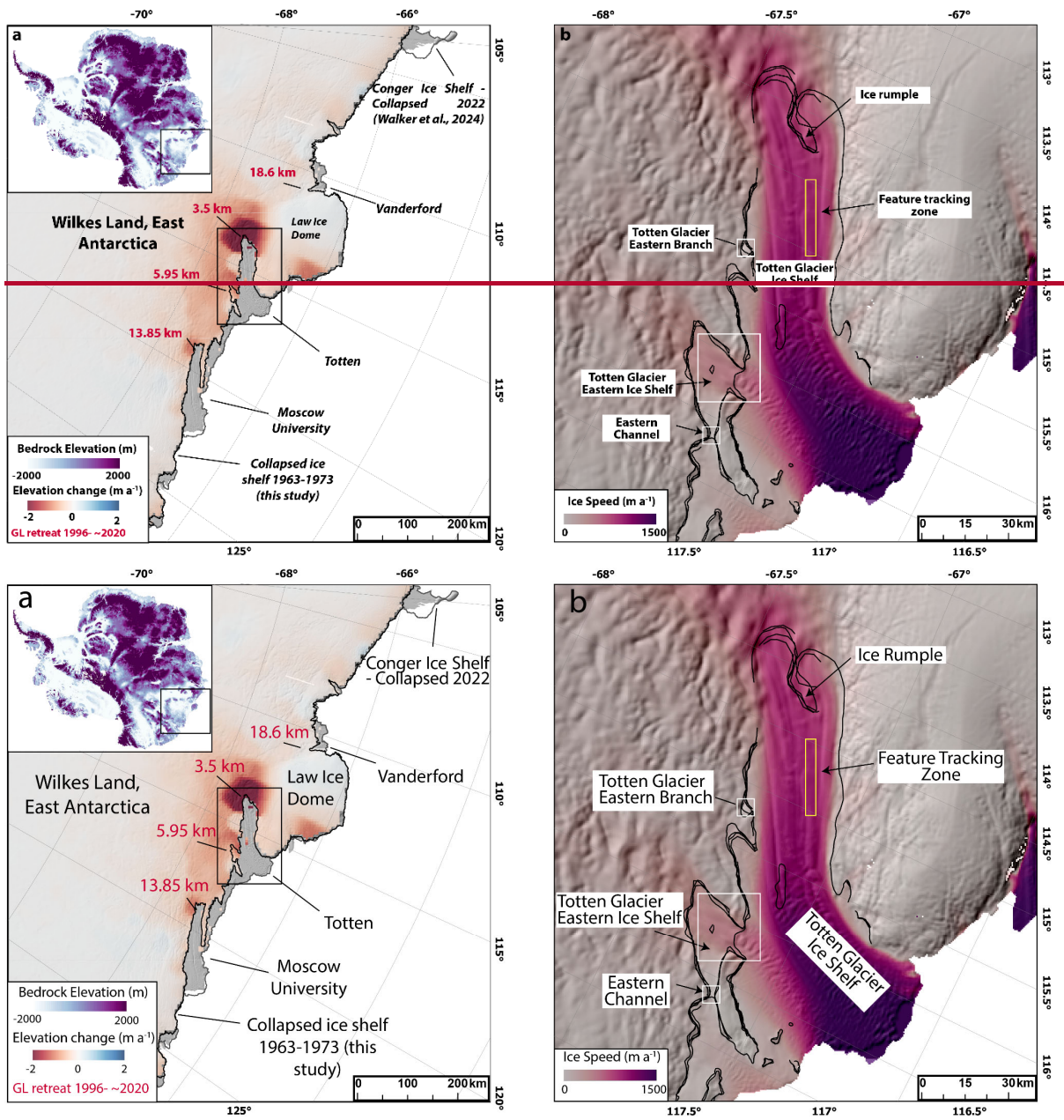
Figure 1: a) Ice-surface elevation change in Wilkes Land, East Antarctica between 2003 and 2019 (Smith et al., 2020), ~~and~~ with ~~rate of~~ grounding-line retreat (1996~2020) of key outlet glaciers from published studies referenced in the main text annotated in red text. The black line ~~on both images~~ is the MODIS 2009 grounding line (Haran, 2021; Scambos et al., 2007). The inset is bed topography from BedMachine (Morlighem et al., 2020). **b)** Ice speed of Totten system with various InSAR derived grounding lines from 2017-2019 (Floricioiu, 2021) overlain. The yellow box represents the region of manual feature tracking. The white boxes are the regions where grounding line migration is mapped. The background image in both panels is the REMA DEM (Howat et al., 2019).

2. Methods

2.1 Satellite imagery

100   The earliest available satellite imagery of Totten glacier system including the ice shelf
101   comprises a pair of ARGON images from 1963 (Fig. 2a). We use the orthorectified and
102   enhanced ARGON imagery of Totten Ice Shelf developed in previous studies (Li et al., 2023a;
103   Ye et al., 2017). The image covering the lower half of the ice shelf and the ice front is of high
104   quality, thus enabling us to identify larger crevasses and surface features. However, the image
105   covering the upper half of the ice shelf and grounding line is of relatively poor quality and the
106   identification of surface features is ~~more~~ challenging (Fig. 2a). For 1973 and 1989, we use the
107   geo-corrected, cloud-free scenes of Totten Ice Shelf acquired respectively by Landsat-1 and
108   Landsat-4 (Miles and Bingham, 2024). Throughout the 2000s, we were able to exploit more
109   regular imagery from Landsat 7, 8 and 9 (Fig. 2). Sporadic SAR imagery is available
110   throughout the 1990s (e.g. ERS), but was not used in this study because we are mainly
111   interested in surface features on Totten Ice Shelf which can express very differently between
112   SAR and optical imagery.

113
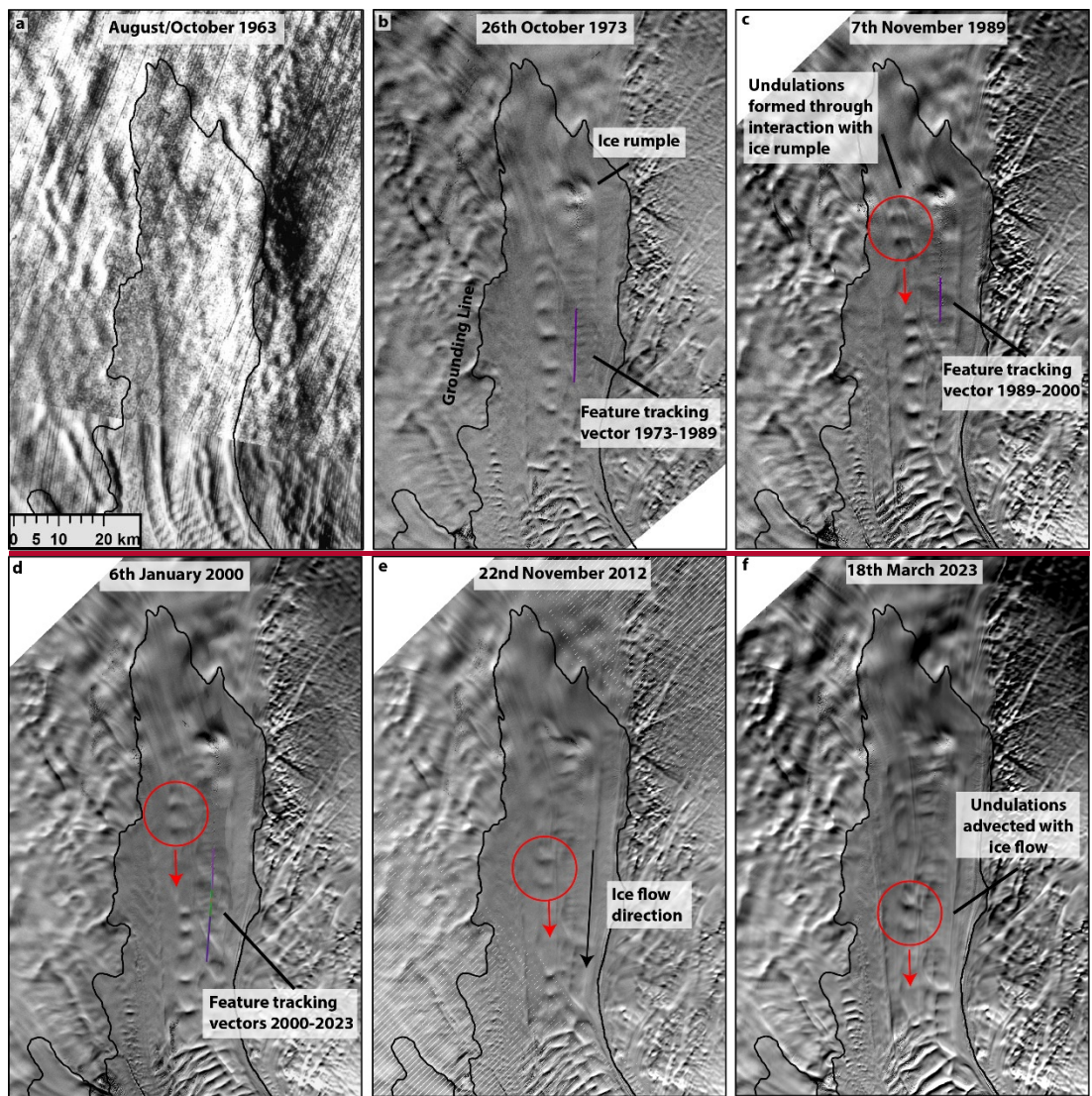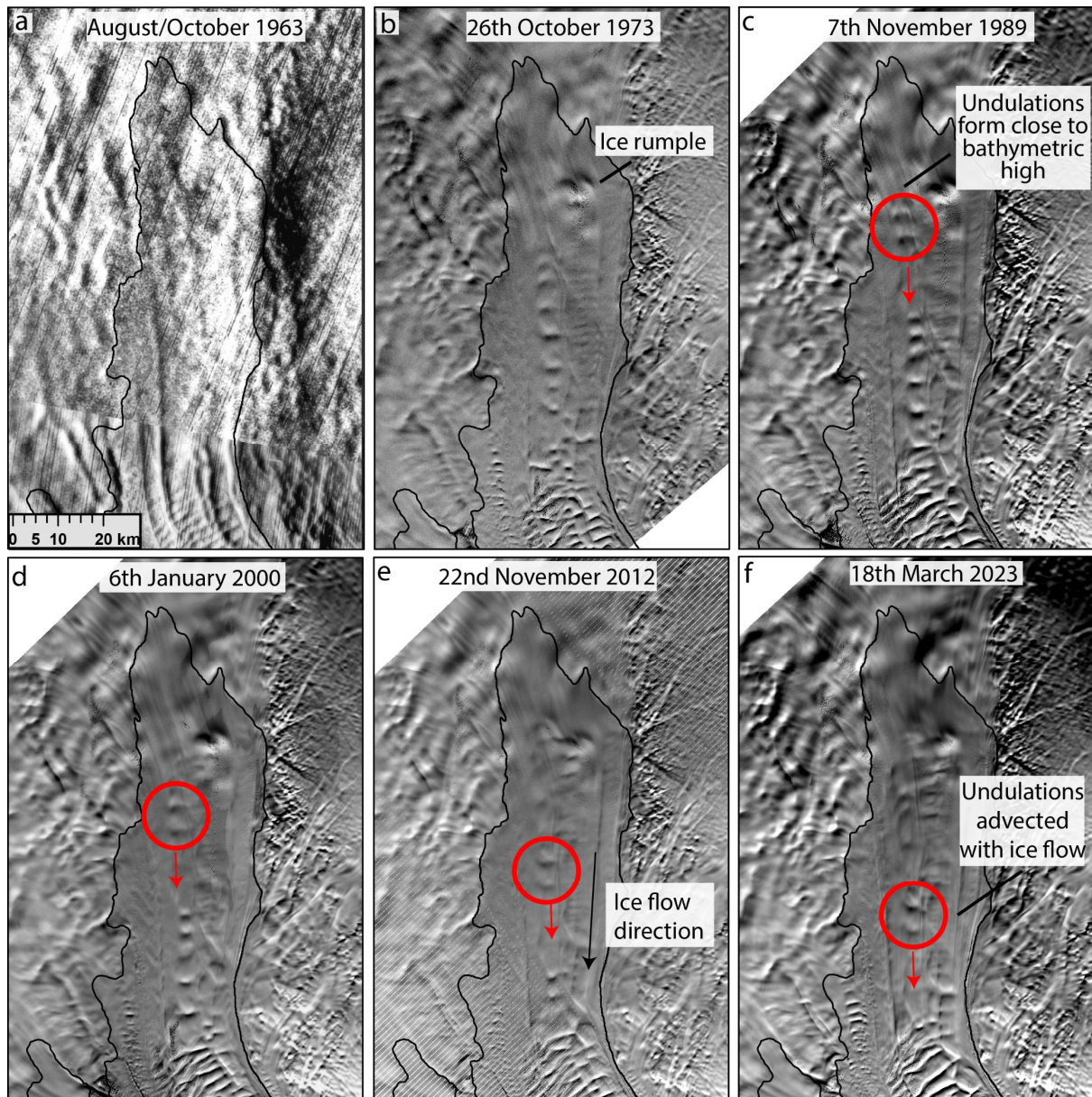
Figure 2: Six decades of satellite imagery over Totten Ice Shelf. The red circles highlight surface undulations forming near ~~the ice rumple inthe~~an ice rumple (location annotated in panel b) in 1989, before being advected downstream with ice flow. ~~Feature tracking vectors used to calculate ice-speed anomalies are shown.~~ARGON (a) and Landsat (b-f) images are courtesy of the U.S. Geological Survey. Black line shows MODIS 2009 grounding line (Haran, 2021; Scambos et al., 2007).

2.2 Ice Speed

Sporadic and lower quality satellite imagery from before 2000 ~~makes~~ make it difficult to determine long-term trends in ice speed at the Totten system. There are two principal reasons for this~~:~~. Firstly, post-2000 ice-speed records show large interannual variability, with ice speeds varying by ~10% over the course of a few years (Greene et al., 2017; Miles et al., 2022). In the absence of continuous observations in the past, it is difficult to determine whether any apparent changes in ice speed from isolated observations in the past (e.g. 1973, 1989) are related to long-term trends or part of this cyclic interannual variability. Secondly, sparse image availability means that uncertainties can be very high. For example, the only pair of Landsat

images covering Totten Glacier between 1975 and 1998 comprises Landsat-4 images from 28th March 1989 and 7th November 1989. During this relatively short period, ice in the yellow box (Fig. 1b) may have only flowed ~700 m and, assuming a displacement uncertainty of ±60 m or 2 pixels (1 for co-registration; 1 for feature tracking), this equates to uncertainties of around ±9%. This very high uncertainty could partly explain the vast range (>20%) of ice-speed anomaly estimates for Totten Glacier in 1989 reported in previous studies (Li et al., 2023a; Li et al., 2015; Rignot et al., 2019; Roberts et al., 2018).

To address both of these issues, we manually track surface features on Totten Ice Shelf using image pairs separated by much longer periods of time (>10 years), which both smooths the impact of interannual variability and reduces relative feature tracking uncertainties because surface features are travelling much greater distances. For example, between 1973 and 1989 we track a 16.07 km displacement of a surface feature and, assuming a displacement uncertainty of two pixels or 120 m (60 m pixel size for Landsat-1), this equates to a smaller uncertainty of ±0.74% (Fig. 3). The disadvantage of this method is that very few surface features remain visible over this length of temporal separation and the process of tracking features over long periods of time can systematically overestimate ice-flow speed if ice does not flow in a straight line (Li et al., 2022). After a careful inspection of the imagery, we focus our feature tracking on one prominent feature, of unknown origin, that repeatedly forms around 20 km downstream (Location; yellow box, Fig. 1b) of the grounding line, and is the only feature that unambiguously maintains its shape and structure for multiple decades (Fig. 3). ~~The close proximity to the grounding line of the surface feature and the confined nature of Totten Ice Shelf means the relative speed anomalies likely provide a good proxy for changes in ice speed across the grounding line, as well as the changes in ice discharge of Totten Glacier. Secondly, because ice flows in a straight line in this region, velocity overestimate corrections are not required.~~ We report changes in ice speed in each epoch as an anomaly with respect to the MEaSUREs ice-velocity reference mosaic of Antarctica (Rignot et al., 2011). This is because, in each epoch, the location of the feature that is tracked starts in a slightly different position. All relative anomalies are calculated along the same flowline and the maximum distance between the centre point of any two anomalies is <20 km. Therefore, given their close proximity it is reasonable to infer that the anomalies are closely comparable to each other through time. In total we measure decadal ice-speed anomalies from 10 epochs detailed in Table 1.

We also calculate interannual ice-speed anomalies at Totten Ice Shelf from 1989 to 2023 where there is a greater availability of satellite imagery (Table 2). We calculate interannual ice-speed anomalies by manually tracking the same surface feature used in decadal ice-speed anomalies. To investigate whether ice-speed anomalies within the feature-tracking zone serve as reasonable proxies for ice-speed anomalies at the grounding line, we use the MEaSUREs annual velocity mosaics (Mouginot et al., 2017). We compare ice-speed anomalies within the feature-tracking zone to ice-speed anomalies within a ~15×5 km bounding box at the grounding line (Fig.~~ure~~ 5) in all years ~~where~~for which data ~~is~~are available in both locations (2008–2009, 2009–2010, and 2013–2020).

173

174

175

176

177

178

179   **Table 1:** Feature tracking - decadal ice-speed anomalies

Image 1	Image 2	Days	Distance (km)	Average speed (m a^{-1})	MEaSUREs speed (m a^{-1})	Anomaly (%)	Uncertainty (km)	Uncertainty (%)
26/10/1973	07/11/1989	5856	16.07	1002	976	2.7	0.12	0.75
07/11/1989	06/01/2000	3712	9.54	938	947	-1.0	0.06	0.63
06/01/2000	03/12/2010	3984	10.70	980	974	0.6	0.03	0.28
22/12/2002	22/11/2012	3623	10.01	1008	981	2.8	0.03	0.30
22/11/2006	25/11/2016	3656	10.07	1005	997	0.8	0.03	0.30
09/11/2007	25/09/2017	3608	9.89	1003	999	0.4	0.03	0.30
29/12/2008	17/12/2018	3640	9.98	1001	1005	-0.4	0.03	0.30
14/11/2009	30/08/2019	3576	9.83	1003	1009	-0.6	0.03	0.31
03/12/2010	19/10/2020	3608	9.88	999	1015	-1.6	0.03	0.30
17/11/2013	24/03/2023	3414	8.86	947	959	-1.3	0.03	0.34

180

181

Within the figure:

26th October 1973

Distance = 16.07 km
Average Speed = 1002 m a^{-1}
Average MEaSUREs speed = 976 m a^{-1}
1973-1989 speed = +2.7% anomaly

Feature remains visible over 16-year time seperation
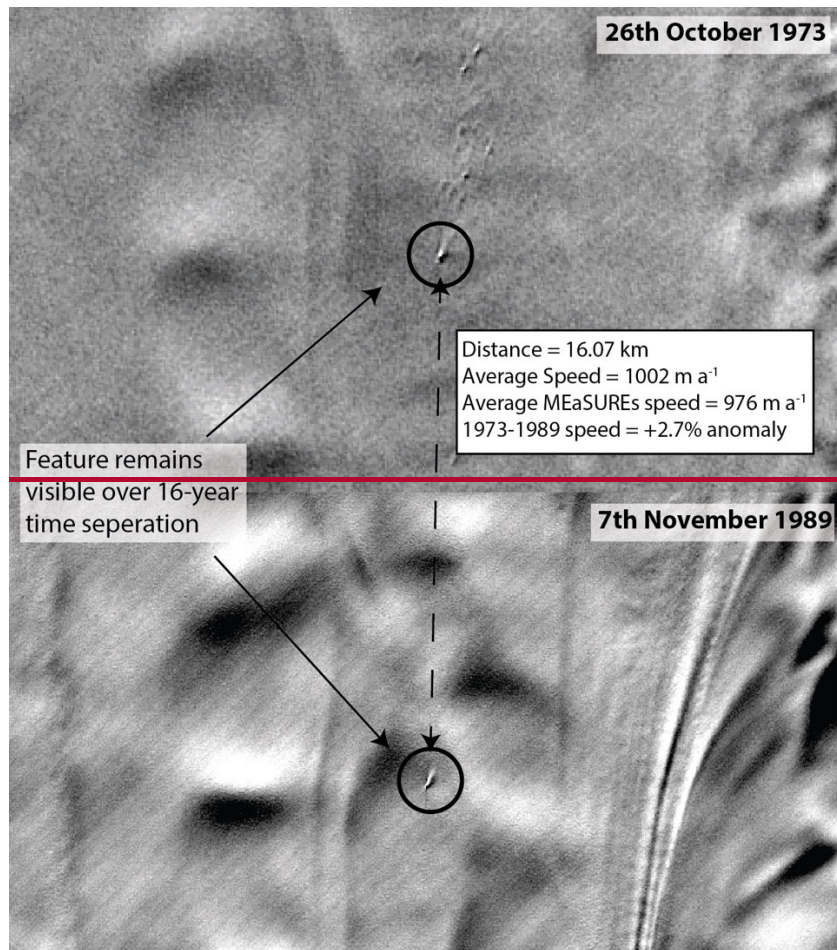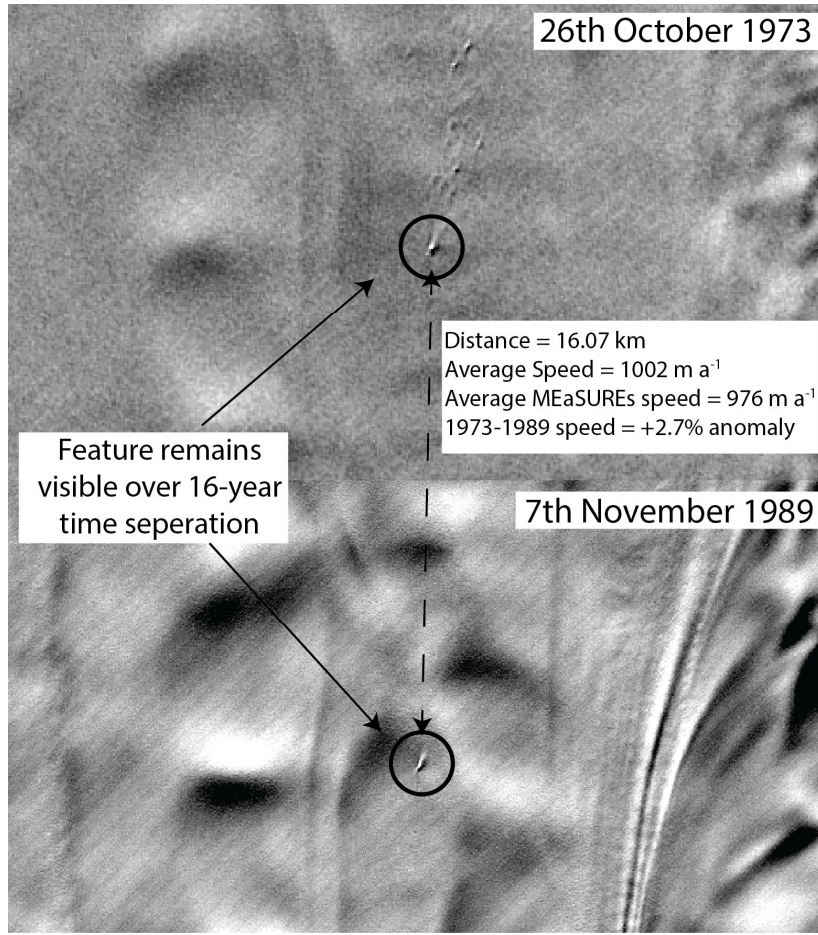
7th November 1989

Figure 3: Image split showing an example of manual feature tracking from a Landsat-1 image from 26th October 1973 to a Landsat-4 image from 7th November 1989. See Figure S1 for more examples. Landsat images are courtesy of the U.S. Geological Survey.

~~In addition to decadal ice-speed anomalies, we also calculate interannual ice-speed anomalies at Totten Ice Shelf from 1989 to 2023 where there is a greater availability of satellite imagery. We calculate interannual ice-speed anomalies by manually tracking the same surface feature used in decadal ice-speed anomalies. We chose this method instead of using the existing ITS_LIVE and MEaSUREs annual mosaics because a preliminary analysis showed these two datasets have large differences in the magnitude of ice speed and interannual trends. In total, we measure interannual ice-speed anomalies from 11 epochs detailed in Table 2.~~

Table 2: Feature tracking - interannual ~~ice~~ ice-speed anomalies

Image 1	Image 2	Days	Distance (km)	Average speed (m a^{-1})	MEaSUREs speed (m a^{-1})	Anomaly (%)	Uncertainty (km)	Uncertainty (%)
28/03/1989	07/11/1989	224	0.69	1124	1004	12.0	0.06	8.70
06/01/2000	22/12/2002	1081	2.76	931	963	-3.3	0.03	1.09
22/12/2002	22/11/2006	1431	3.85	981	971	1.0	0.03	0.78
22/11/2006	29/12/2008	768	2.14	1017	980	3.8	0.03	1.40
29/12/2008	03/12/2010	704	1.98	1029	985	4.5	0.03	1.51
03/12/2010	22/11/2012	720	2.00	1014	1000	1.4	0.03	1.50
22/11/2012	19/10/2014	696	1.85	972	1005	-3.3	0.03	1.62
19/10/2014	25/11/2016	768	2.10	998	1016	-1.8	0.03	1.43
25/11/2016	17/12/2018	752	2.06	1001	1024	-2.2	0.03	1.45
17/12/2018	19/10/2020	672	1.89	1026	1034	-0.8	0.03	1.59
19/10/2020	18/03/2023	880	2.52	1046	1044	0.2	0.03	1.19

194

2.3 Grounding Line

196 We use Landsat imagery to map the break-in-slope (Christie et al., 2016; Fricker et al., 2009),
197 a proxy for the grounding-line location. Our analysis is limited to three locations where we
198 observe clear breaks-in-slope, which are the Totten Glacier Eastern Branch, Totten Glacier
199 Eastern Ice Shelf and the Eastern Channel (Fig. 1b). In these regions, breaks-in-slopes are a
200 good representative for the true grounding line and have been previously used in analysing the
201 ~~basal~~ basal-melting regimes in Totten Ice Shelf due to warm ocean water intrusions
202 (Greenbaum et al., 2015; Li et al., 2023b). We ~~did~~ do not map the grounding line ~~at the main~~
203 ~~glacier trunk of the Totten Ice Shelf featured by~~across Totten Glacier's main trunk over which
204 ~~fast ice flow, where~~ice flow is fast and consequently the break-in-slope is an unreliable proxy
205 for the actual grounding line, and ~~the grounding~~ grounding-line detection is also challenging
206 using DInSAR interferograms or ~~satellite~~ satellite-altimetry datasets (Li et al., 2015; Li et al.,
207 2023b). We map the break-in-slope in each location in 1973, 1989, 2000 and 2023. Based on
208 previous studies, we prescribe a mapping uncertainty of 1 pixel (Christie et al., 2016), along
209 with an additional 1 -pixel uncertainty associated with image co-registration.

2.4 Surface Undulations

211 Surface undulations downstream of bedrock obstacles on floating ice shelves are common
212 features observed across several ice shelves, with prominent examples expressed on Filchner-
213 Ronne (Brunt et al., 2011), Pine Island (Bindschadler et al., 2011), Thwaites (Kim et al., 2018),
214 Totten (Roberts et al., 2018), and Ross (Lee et al., 2012) ice shelves. As ice flows over bedrock
215 obstacles, the topographic variability of the bedrock surface is transmitted to the glacier surface
216 (De Rydt et al., 2013; Gudmundsson, 2003). If the thickness of floating ice varies over time in
217 response to time-varying basal-melt rates, the degree of contact with the underlying bedrock
218 obstacle will also change, resulting in variable imprints on the surface topography of the ice
219 shelf that are subsequently transported downstream with ice flow ~~(Fig. 4)~~.

Sporadic trains of surface undulations form on Totten Ice Shelf ~~adjacent~~ close to a large ice rumple near the grounding line (Fig. 2; Animation S1). These features have been hypothesised to develop in response to time-varying basal-melt rates, whereby lower melt rates lead to enhanced grounding on a bathymetric high, a reduction in ice speed, and the formation of undulations (Roberts et al., 2018) ~~(Roberts et al., 2018); Fig. 2; Animation S1)~~. An inspection of our cloud-free Landsat imagery spanning 50 years reveals that the trains of undulations persist relatively unchanged in shape for ~45 km downstream of the ice rumple as they are advected with ice flow. Therefore, in our earliest cloud-free image from 1973, visible surface undulations at the furthest point downstream of the ice rumple formed decades earlier (Fig. 4) and our full time series provides a near century-long insight into surface-undulation formation.

To further investigate ~~the~~ how the surface undulations form on Totten Ice Shelf, we first measure surface-elevation anomalies from ICESat-2 repeat tracks across the ice shelf to capture the dimensions of the undulations as they are advected downstream with ice velocity (Li et al., 2023b). We use the ICESat-2 ATL06 dataset for Track 26 between May 2019 and November 2023. The ICESat-2 data are applied using the 'ATL06_quality_summary' flag to remove poor-quality elevation measurements possibly caused by clouds or high surface roughness (Smith et al., 2019). They are further corrected for the ocean tide and ocean-loading tide, as well as inverted barometer effects (DAC). Instead of using the ocean-tide correction values generated from the GOT4.8 model that are provided in the ATL06 data product, we use the CATS2008 tidal model to estimate the ocean-tide corrections (Padman et al., 2002). Elevation anomalies are calculated by subtracting a reference elevation profile, defined as the average elevation, from each individual repeat track elevation profile. We also calculate anomalies in the rate of grounded-ice thinning over a 5-year rolling window within a 40 x 40 km box upstream of the grounding line from 1985-2019, using the Antarctic Ice Sheet Elevation Change data (Nilsson et al., 2022) provided by the NASA MEaSUREs ITS_LIVE project (Nilsson et al., 2025). To calculate surface mass balance anomalies between 1979 and 2024, we use the Regional Atmospheric Climate Model (RACMO), version 2.4p1 (Van Dalum et al., 2025). For basal-melt variability, we use the in situ basal-melt time series (2017–2019) derived from autonomous phase-sensitive radar (TI04 – Vaňková et al., 2023), located 5 km upstream of the region where surface undulations form. To examine where surface undulations form in relation to bathymetric highs, we use two bathymetry products. First, we use BedMachine (Morlighem et al., 2020), which incorporates the Greenbaum et al. (2015) bathymetry model as its basis at Totten. Second, we use the updated bathymetry model of Vaňková et al. (2023), which includes additional gravimetry and seismic surveys near the grounding line. We examine both datasets because of subtle differences in bathymetry near the region where surface undulations develop.

We then create a time series of surface-undulation formation by estimating the date on which each undulation formed at the ice rumple. This is estimated by calculating the average flow speed from the MEaSUREs ice-velocity mosaic of Antarctica along a flowline from the ice rumple to 45 km downstream, which represents the region where surface undulations are visible before they are lost to a crevasse field. However, because melt rates are highest near the grounding line (Adusumilli et al., 2020), it is the cumulative melt as ice travels downstream from the grounding line that determines the thickness of ice as it flows over the ice rumple (Fig. 4). Therefore, we also estimate the date on which ice flowed over the grounding line by calculating the average flow speed from the MEaSUREs ice-velocity mosaic of Antarctica along a flowline from the grounding line to the ice rumple.
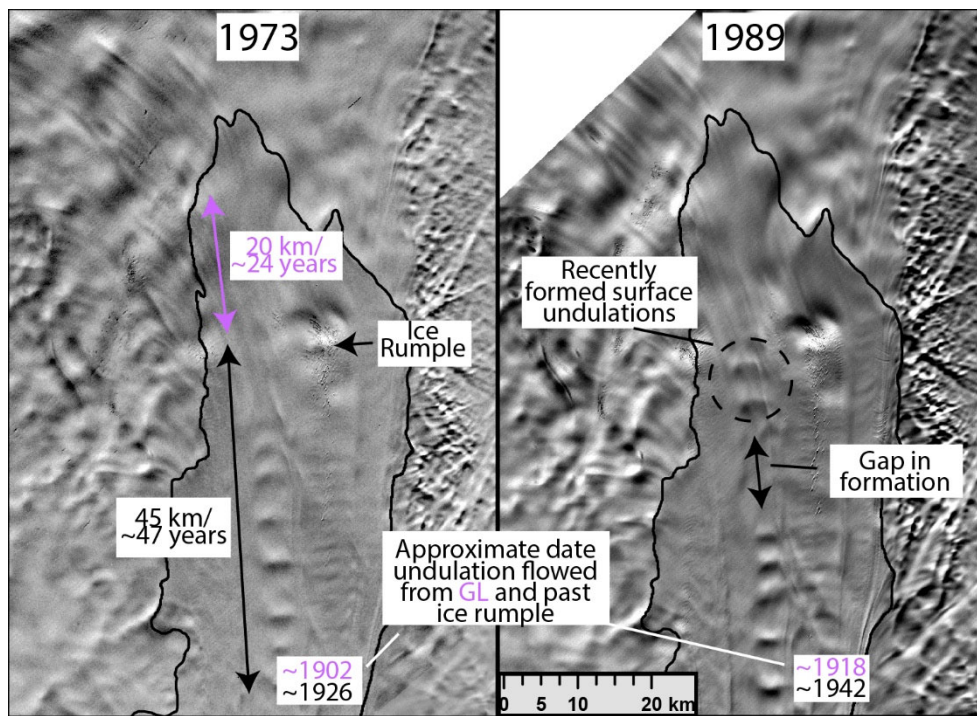
Figure 4: Landsat imagery from 1973 and 1989 showing the time taken for ice to flow from the grounding line to the ice rumple and the from the ice rumple to the most distant surface undulation.
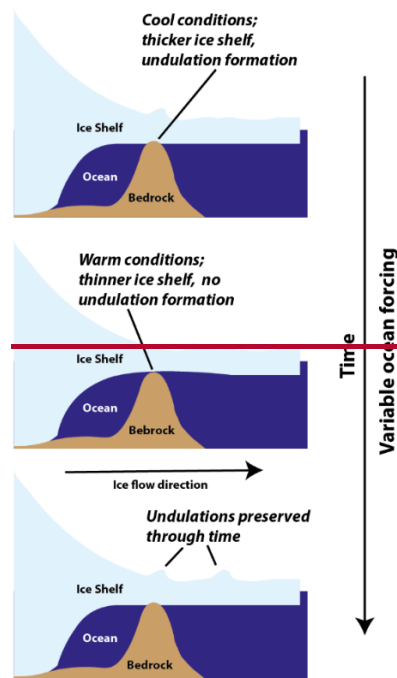
Landsat images are courtesy of the U.S. Geological Survey

~~**Figure 4:** Schematic showing the formation of surface undulations from time-varying melt rates.~~

3. Results

3.1 Ice Speed

Ice-speed anomalies within the feature-tracking zone on Totten Ice Shelf are correlated (~~P~~p-value = 0.02) to ice-speed anomalies at the grounding line (Fig. 5a and b). Therefore, our multidecadal measurements of ice speed derived from the feature-tracking zone 20 km downstream of the grounding line ~~can be considered~~are appropriate proxies for ice speed at the grounding line.

We observe no clear trend in multidecadal ice-speed anomalies at Totten Ice Shelf between 1973 and 2023, with ice-speed anomalies ranging from -1.6 ±0.3% from 2010-2020 to +2.8 ±0.3% from 2002-2012 (Fig. 5). We observe a much greater range of ice-speed anomalies over interannual timescales. We record a maximum ice speed anomaly of +12 ±8.7% in 1989 and a minimum ice speed anomaly of -3.3 ±1.1% from 2000-2002 (Fig. 5). Regular ice-speed measurements between 2000 and 2023 reveal oscillatory behaviour in speed anomalies of up to ~8% over the course of 6-7 year cycles (Fig. 5). There is no evidence of a sustained speed-up of Totten Glacier over the past 50 years.

287

288
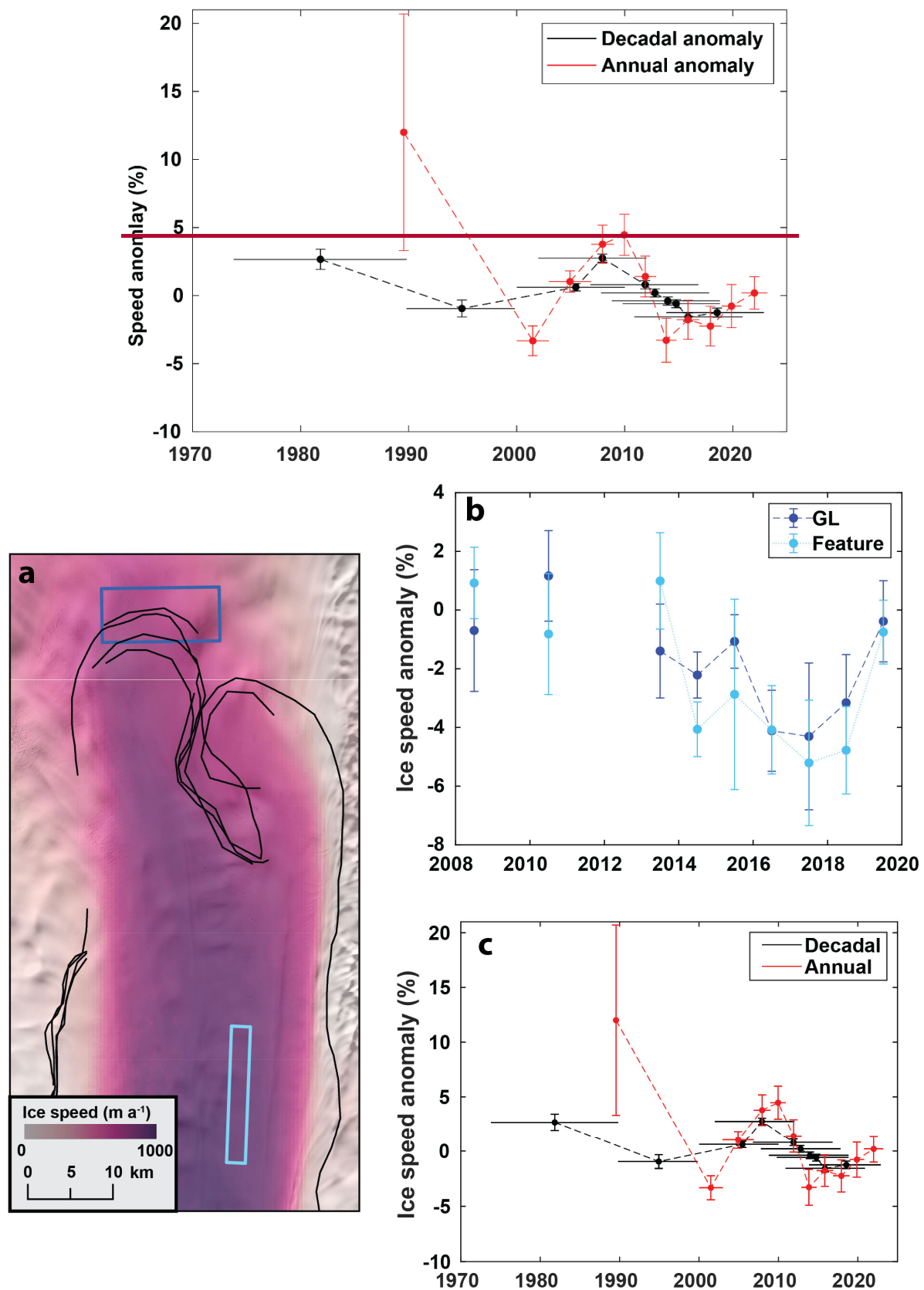
Figure 5: Ice-speed anomalies at Totten Ice Shelf. **a)** Location of bounding boxes used to extract annual ice‑speed anomalies at the grounding line (blue) and feature‑tracking zone (light blue), with ice speed from the MEaSUREs ice velocity mosaic and grounding lines derived between 2017 and 2019 overlain (Floricioiu, 2021). **b)** Annual ice‑speed anomalies from the MEaSUREs annual mosaics. **c)** Decadal

293 and annual ice-speed anomalies extracted manually from within the feature box. Black data points
294 represent decadal ice-speed anomalies; red data points represent the interannual ice-speed anomalies.
295 Horizontal lines represent the time gap between the two images used to track surface features.

3.2 Grounding Line

297 At the Totten Glacier Eastern BranchBranch, we observe a maximum 4.1 ± 0.12 km grounding-
298 line retreat between 1973 and 2023, that includes a 0.8 ± 0.12 km maximum retreat between
299 1973 and 1989 (Fig. 6a). The width of the mouth of the Totten Glacier Eastern Ice Shelf
300 increased by around 3.8 ± 0.12 km between 1973 and 2023 with retreat on both the northern
301 and southern flanks (Fig. 6b). The rate of retreat is reasonably consistent in each of our three
302 epochs: 1973-1989; 1989-2000 and 2000-2023. At Eastern Channel we observe a gradual
303 widening through each of our 3 epochs, and overall between 1973 and 2023 the channel width
304 approximately doubled (Fig. 6c).

305

306
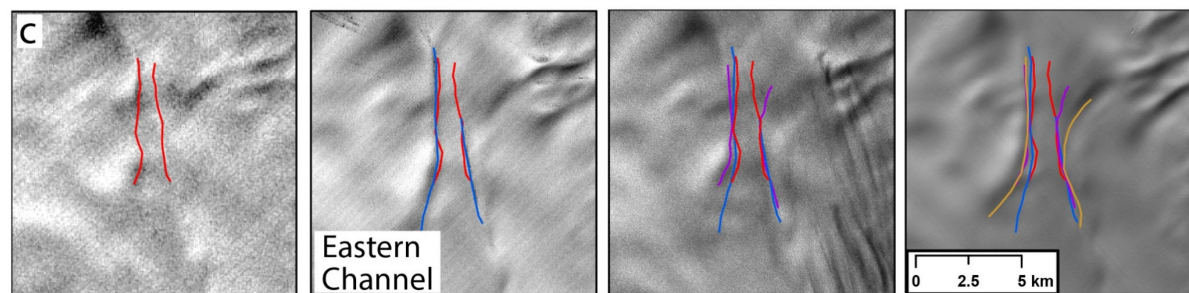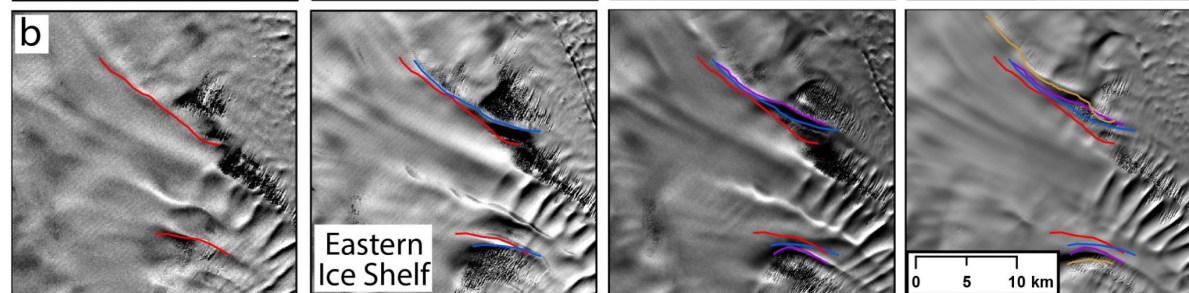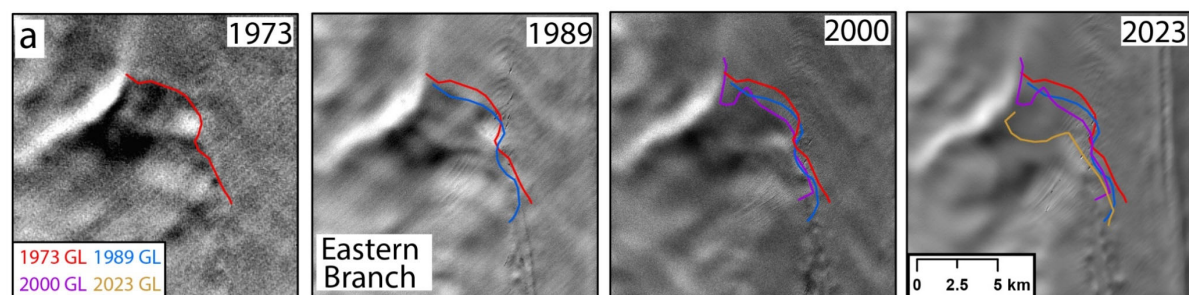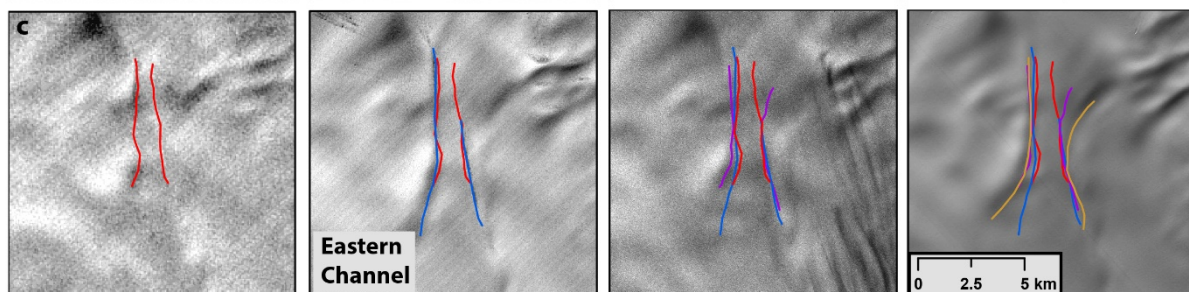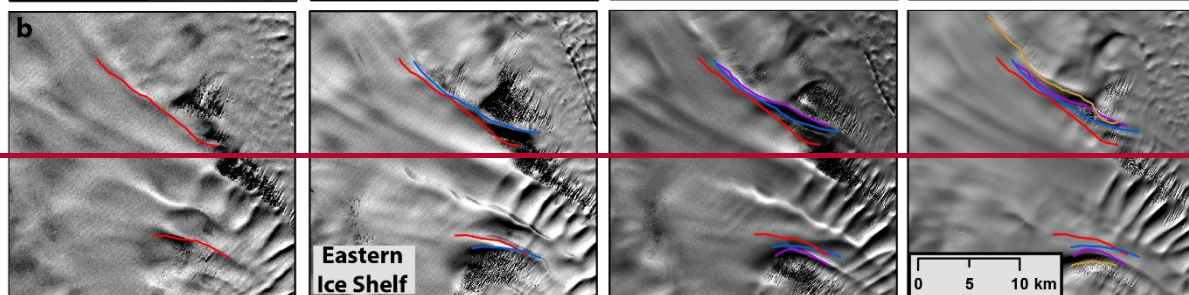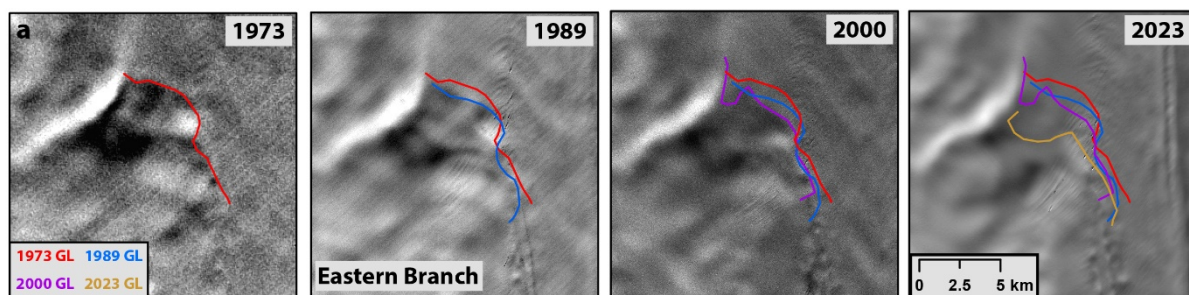
Figure 6: Grounding-line retreat tracked from Landsat imagery for **a)** Eastern Totten Ice Shelf, **b)** Eastern Ice Shelf and **c)** Eastern Channel. ~~See Figure 1b for locations~~The(-location of each ~~section~~panel is shown ~~in the~~as white boxes in Fig~~ure~~. 1b). Landsat images are courtesy of the U.S. Geological Survey.

3.3 Surface Undulations

3.3.1 Surface–undulation formation

ICESat-2 repeat tracks across a prominent surface undulation as it flows downstream show a surface ~~height~~elevation change of up to 25 m over three years, or approximately 8 m a^{-1} (Fig. 7d). The magnitude of this elevation anomaly is broadly comparable to in situ estimates of basal--melt variability (~9 m a^{-1}), measured 5 km upstream of the location where the surface undulations form (Fig. 7e). Between 1985 and 2019, grounded ice within a 40 × 40 km bounding box immediately upstream of the grounding line thinned at an average rate of approximately 1 m a^{-1}, with interannual variability typically within ±0.5 m a^{-1} (Fig. S2). Mean surface mass balance between 1979 and 2024 is approximately 1 m a^{-1}, with interannual variability in the range of ±0.4 m a^{-1} (Fig. S3).

Figure 7: a) Landsat-8 image from 17th November 2013 showing recently forming surface undulations. The white box is the inset for the zoomed ~~in image on the~~inset, bottom left. The purple transect represents the profile of the ICESat-2 repeat tracks. **b)** Vaňková et al. (2023) bathymetry. **c)** BedMachine bathymetry (Morlighem et al., 2020). The dotted lines on panels a-c represent flow lines of the surface undulations, the red circle represents the location where surface undulations are first visible in optical imagery, and the black lines are grounding lines derived between 2017 and 2019 (Floricioiu, 2021). **d)** Repeat ICESat-2 tracks over Totten Ice Shelf highlighting the surface-elevation anomalies associated with the surface undulations as they flow downstream. **e)** In situ basal-melt timeseries from Vaňková et al. (2023) located at the red star.

3.3.2 Surface-undulation timeseries

Based on the average flow speed of 950 m a⁻¹ along the transect of the surface undulations, and assuming ice-flow speed has remained constant through time, the most distant surface undulation 45 km downstream of the ice rumple will have formed ~47 years before the image date (Fig. 4~~7b~~). We also calculate that it takes approximately 24 years for ice to flow from the

grounding line to the ice rumple based on an average flow speed of 850 m a^{-1} (Fig. 4). This means that in our earliest Landsat image in 1973, the most distant surface undulation will have formed in approximately 1926, being imprinted into ice that had crossed the grounding line in approximately 1902 (Fig. ~~4~~7b). The time series of surface-undulation formation reveals three distinct ~~phases~~ phases of ~~surface~~ surface-undulation formation over the past 100 years (Fig. 8~~7c~~). For simplicity, we define the start and end point of each phase by the dates on which ice crossed the ice rumple, but note that these dates would be shifted ~20 years earlier in time if the phases were defined by the dates on which the same ice crossed the grounding line. The first phase is characterised by regular surface-undulation formation at the ice rumple between ~~1926~~ 1920 and 19~~65~~65~~, imprinted into ice that had flowed across the grounding line from 1902-1941.~~. The second phase is characterised by a gap in surface-undulation formation between ~~1965~~ 1965 and 19~~80~~80~~, for ice that had flowed across the grounding line from 1941-1961.~~. The ~~final~~ third phase is characterised by intermittent formation of surface undulations between ~~1985~~ 1980 and 20~~20~~23. ~~, imprinted into ice that had flowed across the grounding line from 1961-1999.~~ Notably, surface undulations in this final phase appear to reduce progressively in size, possibly implying a progressive thinning of the ice shelf.
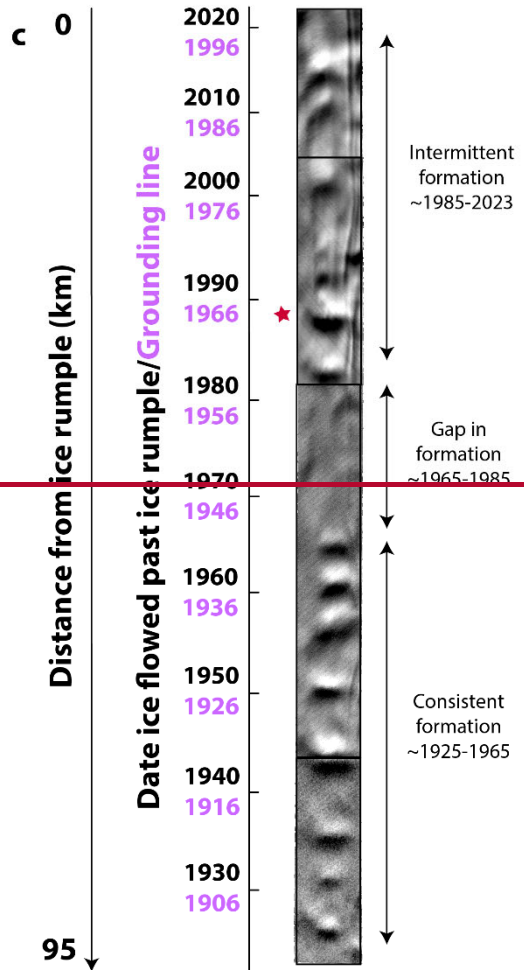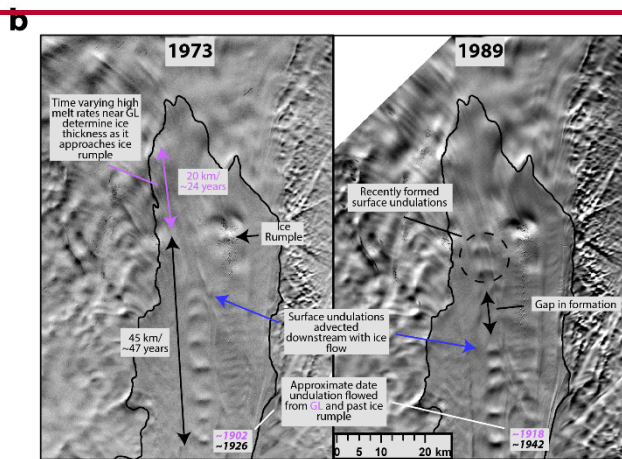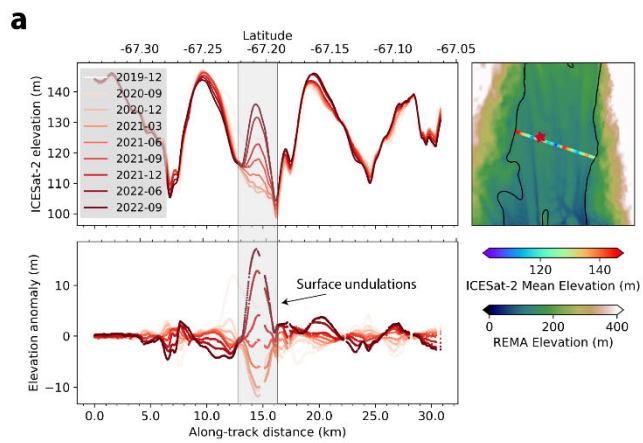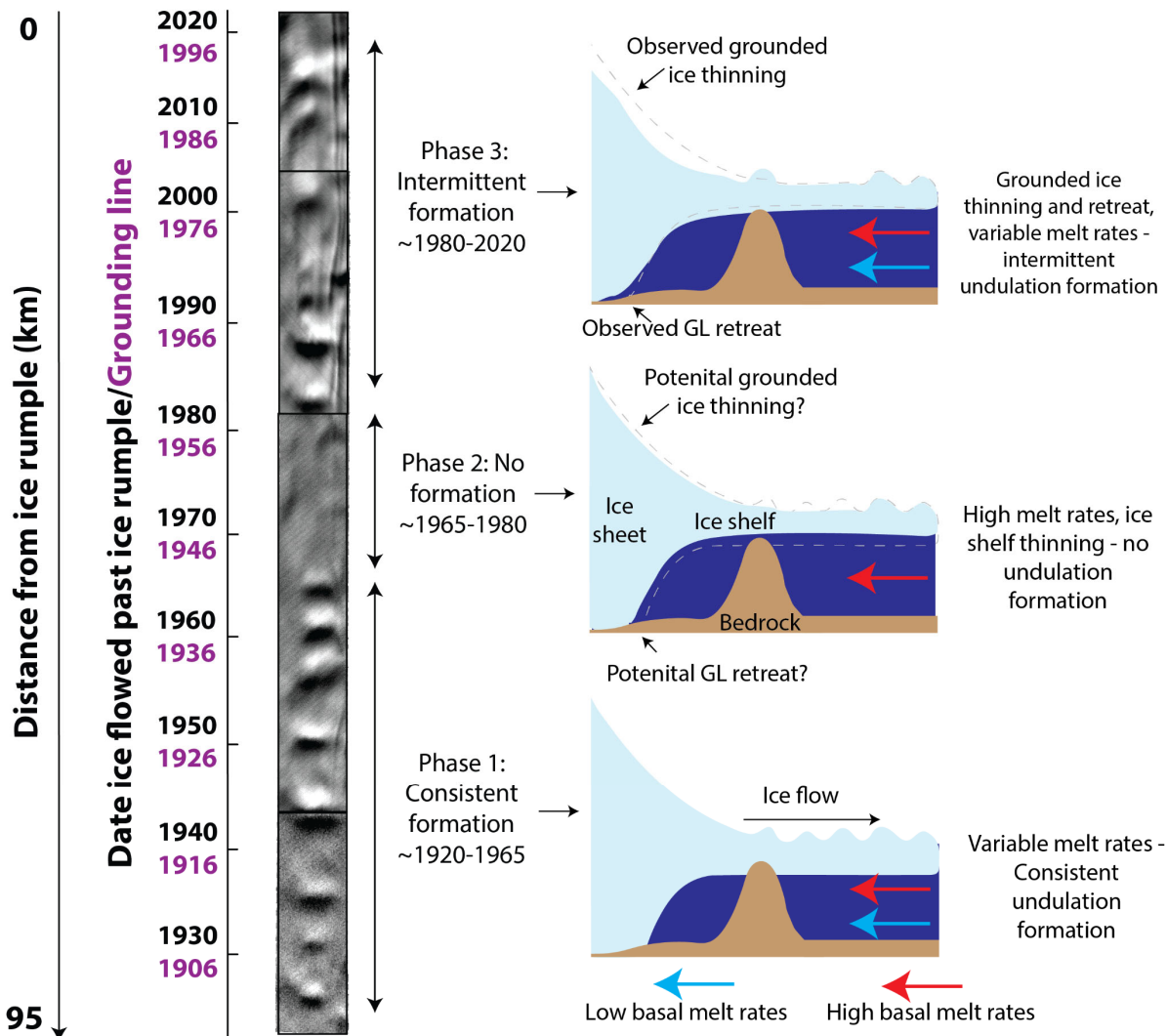
Figure 8~~7~~: ~~a) Repeat ICESat-2 tracks over Totten Ice Shelf highlighting the surface elevation anomalies associated with the surface undulations as they flow downstream. Grey box marks the location of the surface undulations and the height change represents the downstream advection of the undulations b) Landsat imagery showing surface-undulation advection downstream. The black line on both images is the MODIS 2009 grounding line (Haran, 2021; Scambos et al., 2007). c)~~ Time series of surface-undulation formation comprised of four Landsat images (1973, 1989, 2000 and 2023) stitched together~~, the boundary of each image is denoted by the black boxes~~ (image boundaries denoted by black boxes). ~~The red star represents the surface undulation profile depicted in panel a. Landsat images are courtesy of the U.S. Geological Survey.~~The time series is separated into three phases, with a corresponding schematic showing the processes driving surface-undulation formation.

4. Discussio~~n~~n

4.1 No speed-up of Totten Glacier since at least 1973

Our results show that there has been no clear multidecadal trend in ice speed at Totten Ice Shelf from 1973-2023 (Fig. 5)~~, meaning~~implying that there ha~~s~~ve also been no sustained changes ~~in~~to ice--shelf buttressing. ~~Assuming that ice-speed anomalies in the locations we tracked on the ice shelf (Fig. 1a) are good proxies for ice speed at the grounding line, T~~this means that

average ice discharge has likely remained relatively unchanged at Totten Glacier over the past 50 years, despite strong interannual variability. Although there exists some interdecadal variability in snowfall (Kim et al., 2024), there is no evidence for any long-term trends in snowfall from the nearby Law Dome ice core (Jong et al., 2022; Roberts et al., 2015) and, because Totten's present ice discharge outweighs input from snowfall, this means that the Totten catchment was likely losing a similar amount of mass from 1973-1989 in comparison to the 2000s. Thus, the trigger for mass loss at Totten catchment predates the onset of the Landsat satellite record.

We note that Li et al. (2023a) reported oninferred a long-term speed up at the Totten grounding line between 1963-1973 and 2022, but with very little change in ice speed 50 km upstream of the ice front over the same time period (Fig. 2; Li et al., 2023a). However, Tthe rate of acceleration in ice speed at the grounding line reported in Li et al. (2023a) was not consistent over this time period, however, with a large ~18% acceleration between 1963-1973 and 1973-1989, then limited change in ice speed between 1973-1989 and 2022. From our methods, we can only reiterate that the Totten system has not experienced any multidecadal acceleration since 1973, because we were unable to track any surface features on the 1963 ARGON image near the grounding line.

4.2 Ongoing grounding-line retreat since at least 1973

Our results show consistent grounding-line retreat at Totten Glacier Eastern Ice Shelf and Totten Glacier Eastern Branch between 1973-1989, 1989-2000 and 2000-2023 (Fig. 6). Our observation that the grounding line was already retreating in regions where the break-in-slope is visible between 1973 and 1989 further supports the notion that the Totten Glacier system was already out of balance and losing mass during this period. The Eastern Channel has also been consistently widening from 1973-1989, 1989-2000 and 2000-2023 (Fig. 6c). This channel, first discovered by radio-echo sounding (Greenbaum et al., 2015), has subsequently been shown to be tidally modulated via satellite-radar interferometry (Li et al., 2023b). The Eastern Channel is important because it may provide a direct pathway for warm mCDW to enter the Eastern Ice Shelf cavity (Greenbaum et al., 2015). The expanding width of the channel since at least 1973 would suggest a greater volume of tidally pumped warm mCDW is being progressively funnelled through this trough into the ice-shelf cavity.

4.3 Surface- undulation formation

Surface undulations on Totten Ice shelf must form in response to an intermittent local re-grounding of ice driven by time-varying basal- melt rates. formust satisfyconditionsThis is because: 1) They form on or downstream of bathymetric highs. 2) Their surface signature is incompatible with other features (e.g., basal crevasses; Luckman et al., 2012; McGrath et al., 2012) that can form downstream of pinning points, and 3) The elevation anomaly associated with the surface undulations broadly matches observations of basal- melt variability (Fig. 7).

The bathymetry near the Totten grounding zone is complex and, despite recent improvements, uncertainties remain (Fig. 7b andversus c). On the basis of the updated seismic- and gravimetry-derived bathymetry of the Totten grounding zone by (Vaňková et al., (2023), surface undulations form in a narrow (3-4 km wide) channel (3-4 km)between theice grounded ice-on the eastern flank of the ice shelf and a secondary bathymetric high point close toupstream of the main ice rumple (Fig. 7b). In this scenario, surface undulations could form during periods

of greater localised re-grounding on the secondary bathymetric high causing a narrowing of the channel. However, an earlier bathymetry product (Greenbaum et al., 2015) ~~inferred~~resolved a much more prominent broad bathymetric ridge directly under the zone of surface-undulation formation (Fig. 7c). ~~Although~~Although the~~The~~ presence of this broad ridge was deemed highly incompatible with the Vaňková solution, ~~but but~~ Vaňková et al. (2023) ~~do do~~ ~~acknowledge~~acknowledged that ~~that some~~uncertainties remain with their more recent product. Therefore, an alternative explanation is that surface undulations form in response to a localised re-grounding on a bathymetric high, smaller in prominence than inferred by the Greenbaum solution, directly underneath where the surface undulations first become visible in optical imagery (Fig. 7).

The surface undulations that we have tracked along Totten Ice Shelf are large features that result in up to 25 m of differential surface-elevation anomalies over the course of three years (Fig. 7d). Thus, their formation requires minimum cyclic variations in ice-shelf thickness of ~~at least~~ 8-9 m a^{-1} in the region where they form. In situ observations of basal-melt rates from autonomous phase-sensitive radars ~5 km upstream of the undulation-formation zone have shown basal-melt variability of around 9 m a^{-1} (Vaňková et al., 2023; Fig. 7e), the magnitude of which compares well to the surface-elevation anomalies of the undulations. Furthermore, because the in situ basal-melt timeseries is short (two years), a greater magnitude of basal-melt variability could be expected in the long-term. In comparison, the interannual variability associated with grounded-ice elevation change and surface mass balance (Fig. S2) is an order of magnitude lower.

The physical mechanism proposed to drive the large interannual variability in basal-melt rates is variability in the depth of the thermocline on the continental shelf (Hirano et al., 2023). Oceanographic profiles have confirmed a two-layered structure of the water column with cold Winter Water overlying warm mCDW, separated by a sharp boundary (Hirano et al., 2023; Nakayama et al., 2023; Rintoul et al., 2016). Updated bathymetry on the continental shelf has shown that the depth of the thermocline between the two water masses broadly matches the depth of the shallowest sill on the Central Totten Trough that funnels warm mCDW towards the ice shelf (Hirano et al., 2023). Therefore, small changes in the depth of the thermocline could cause large differences in temperature of water transported beneath Totten Ice Shelf, driving large variability in basal-melt rates and surface-undulation formation. Repeat oceanographic observations and moorings show variability in thermocline depth on both interannual and tidal timescales, but these observations are limited to just four years (Rintoul et al., 2016; Hirano et al., 2023). However, observations from satellite altimetry since the early 1990s show multi-~~meter~~metre variations in ice-shelf thickness anomalies, the magnitude of which can only be explained by basal-melt variability (Roberts et al., 2018), suggesting that variability in basal-melt rates has persisted for decades. Roberts et al. (2018) calculated that the wavelength (6-7 years) of ice-shelf thickness variations matches the wavelength of the surface undulations in a Landsat-7 image from 2010, further supporting the notion that the surface undulations are formed by time-varying melt rates. A number of different processes could contribute to driving variability in the thermocline depth including variations in Antarctic Slope Current strength (Nakayama et al., 2021), intrinsic variability (Gwyther et al., 2018), zonal wind strength on the continental-shelf break (Greene et al., 2017) and coastal-polynya activity (Gwyther et al., 2014; Khazendar et al., 2013), but the dominant driver remains unclear.

4.43 Change in melt pattern in the mid-20th century Anomalously high basal- melt rates in the mid-20th century

The surface- undulation timeseries provides a novel proxy for basal- melt rates and ice- shelf thickness variability over the past century. In Phase 1, dating from ~1920-1965, surface- undulation formation is consistent (Fig. 8), implying cyclic warm and cool anomalies in basal -melt rates driving intermittent re-grounding on bathymetric highs. In Phase 2, dating from ~1965-1980, no surface undulations form (Fig. 8). This can be explained by a prolonged period of increased basal- melt rates and consequently thinner ice passing over the bathymetric high, possibly driven by a shallowing of the thermocline on the continental shelf. In Phase 3, dating from ~1980-2020, surface undulations form intermittently (Fig. 8). A key implication here is that, on average, melt rates must have been lower during ~1980-2020 (Phase 3) relative to 1965-1980 (Phase 2). This is because surface undulations form in Phase 3 despite ongoing grounded- ice thinning (Fig. S2) causing progressively thinner ice to flow into the ice shelf, meaning that progressively more extreme cool anomalies are required for surface- undulation formation (Fig. 8). There is also the possibility of progressively warmer CDW being fed onto the continental shelf since the early 20th century in response to a wind-driven southward shift of the Antarctic Coastal Current (Herraiz-Borreguero and Naveira Garabato, 2022; Yamazaki et al., 2021). In addition, ~~T~~ the ongoing grounded- ice thinning could explain why surface undulations also appear to be visibly smaller in ~1980-2020 (Phase 3) compared to ~1920-1965 (Phase 1). ~~There is also the possibility of progressively warmer CDW being fed onto the continental shelf since the early 20th century in response to a wind-driven southward shift of the Antarctic Coastal Current (Herraiz-Borreguero and Naveira Garabato, 2022; Yamazaki et al., 2021).~~

~~At Totten Ice Shelf, high basal-melt-rate variability has been observed from autonomous phase-sensitive radars (Vaňková et al., 2023), variable ocean temperatures have been recorded on the nearby continental shelf (Hirano et al., 2023; Nakayama et al., 2023; Rintoul et al., 2016), and variability has been reported in both ice speed (Greene et al., 2017; Miles et al., 2022) and ice-shelf thickness (Adusumilli et al., 2020; Paolo et al., 2015). The surface undulations that we have tracked along Totten Ice Shelf are large features that result in up to 25 m differential surface-elevation anomalies (Fig. 7a). Roberts et al. (2018) calculated that the wavelength (6-7 years) of the surface undulations in a Landsat-7 image from 2010 matched the wavelength of elevation anomalies of the ice shelf observed from satellite altimetry. We estimate that the average length of all visible surface undulations in Landsat imagery dating back to 1973 is similar, at ~5.5 years, based on an average length of ~5 km and an average flow speed of 900 m a⁻¹ at the ice rumple where the undulations form. Independent ocean modelling has shown the dominant intrinsic variability in the melt rates of Totten Ice Shelf occurs over ~3 and ~7 years cycles (Gwyther et al., 2018), broadly matching the wavelength of surface-undulation formation. Taken together, along with evidence from similar features on other ice shelves (Bindschadler et al., 2011, Kim et al., 2018), there is substantial theoretical and observational evidence that the surface undulations are formed by time-varying basal-melt rates. Thus, any substantial change in the pattern of surface-undulation formation at Totten Ice Shelf through time likely relates to changes in contact with the underlying pinning point in response to variability in ice-shelf thickness and basal-melt rates.~~

~~The abrupt switch from regular surface-undulation formation from 1925-1965 to no surface-undulation formation between 1965 and 1985 implies a change in melt rates and ice-shelf~~

thickness (Fig. 7c). Specifically, because the period from 1965-1985 is characterized by a smoother ice-shelf surface, this suggests warmer conditions and a thinner ice shelf with much more limited interaction with the ice rumple during this period. Surface undulations return sporadically between 1985 and 2023, demonstrating a shift to relatively cooler conditions, but the ice shelf may be thinner compared to 1925-1965 when surface undulations formed on a more regular basis (Fig. 7c).

Modern satellite-altimetry observations of ice-shelf thickness change at Totten Ice Shelf support our hypothesis that the absence of surface-undulation formation between 1965 and 1985in Phase 2 represents a period of higher basal-melt rates and a relatively thinner ice shelfpassing over bathymetric high points near the ice rumple. Observations of ice-shelf thickness change between 2003 and 2019 (Smith et al., 2020) shows show a conflicting thickness-change signal across the ice shelf (Fig. 9b8). The upper ice shelf near the ice rumple thickened, while the mid-section of the ice shelf thinned and there was limited change in the lower ice shelf, during this period. This unusual pattern can be explained by the advection of relatively thinner and thicker bands of ice downstream with ice flow. There are two principal reasons supporting this interpretation. First, the length of the core of the thinning section (~20 km) broadly matches the displacement of ice expected over the 16-year time-separation (~16 km) of the ice--thickness--change dataset (Fig. 9b), as well as the length of Phase 2 during which no surface undulations formed (~18 km; Fig. 8). Secondly, the downstream boundary of the thinning section of the ice shelf corresponds directly to the boundary between Phase 1 and Phase 2 of undulation formation, while the upstream boundary of the thinning section corresponds directly to the boundary between Phase 2 and Phase 3 of undulation formation (Fig. 9b). Basal--melt rates are an order of magnitude higher near the grounding line (>50 m yr^{-1}), compared to the mid-ice shelf (~10 m yr^{-1}) (Fig. 9a; Adusumilli et al., 2020). This means that variability in melt rates would be expected to be larger near the grounding line compared to the mid-ice shelf. Therefore during ~1965-1980 (Phase 2) where basal--melt rates were higher and no surface undulations formed, ice will have flowed out of the zone of high basal-melt rates (i.e. grounding zone) relatively thinner, compared to Phase 1 where basal--melt rates were lower and undulations formed consistently. Thus, as the band of ice associated with high basal--melt rates at the grounding line and ice rumple in 1965~1980 flows downstream it will replace relatively thicker ice from Phase 1 causing a thinning signal. A similar process can explain the thickening in the upper ice shelf, relatively cooler melt rates in Phase 3 (~1980-2020) result in thicker ice flowing out of the zone of higher basal--melt rates, replacing the thinner ice associated with Phase 2, causing a thickening signal.

This can be explained by waves of ice thickness variations in response to time-varying basal melt rates near the grounding line being advected downstream with ice flow. Notably, the boundary between thinning and thickening ice derived by satellite altimetry (Fig. 8) corresponds to the boundary between the 1985-2023 and 1965-1985 phases in surface-undulation formation (Fig. 7c). That is, the 2003-2019 thickening of the upper section of the ice shelf can be explained by the relatively thinner ice associated with the 1965-1985 period of no surface-undulation formation and high melt rates being advected downstream and being replaced by relatively thicker ice associated with relatively low melt rates and the 1985-2023 period of intermittent surface-undulation formation. The thinning section of the mid-ice shelf is explained by relatively thick ice associated with the 1925-1965 regular phase of surface-undulation formation being advected downstream and being replaced by relatively thin ice

associated with the 1965-1985 period of no surface-undulation formation.. Therefore, we are confident that the 1965-1985 gap in surface-undulation formation represents a section of relatively thin ice as it flowed over the ice rumple in response to higher basal-melt rates. However, the timing of this period of high melt rates likely predates the 1965-1985 gap in surface-undulation formation. This is because it takes around 24 years for ice to travel from the grounding line to the ice rumple, and it is the cumulative melt rate during this period that determines the thickness of the ice shelf as it crosses the ice rumple. Thus, we estimate that the switch to higher melt rates at the grounding line took place at some point between 1941 and 1965, to which we refer as the mid-20th century.
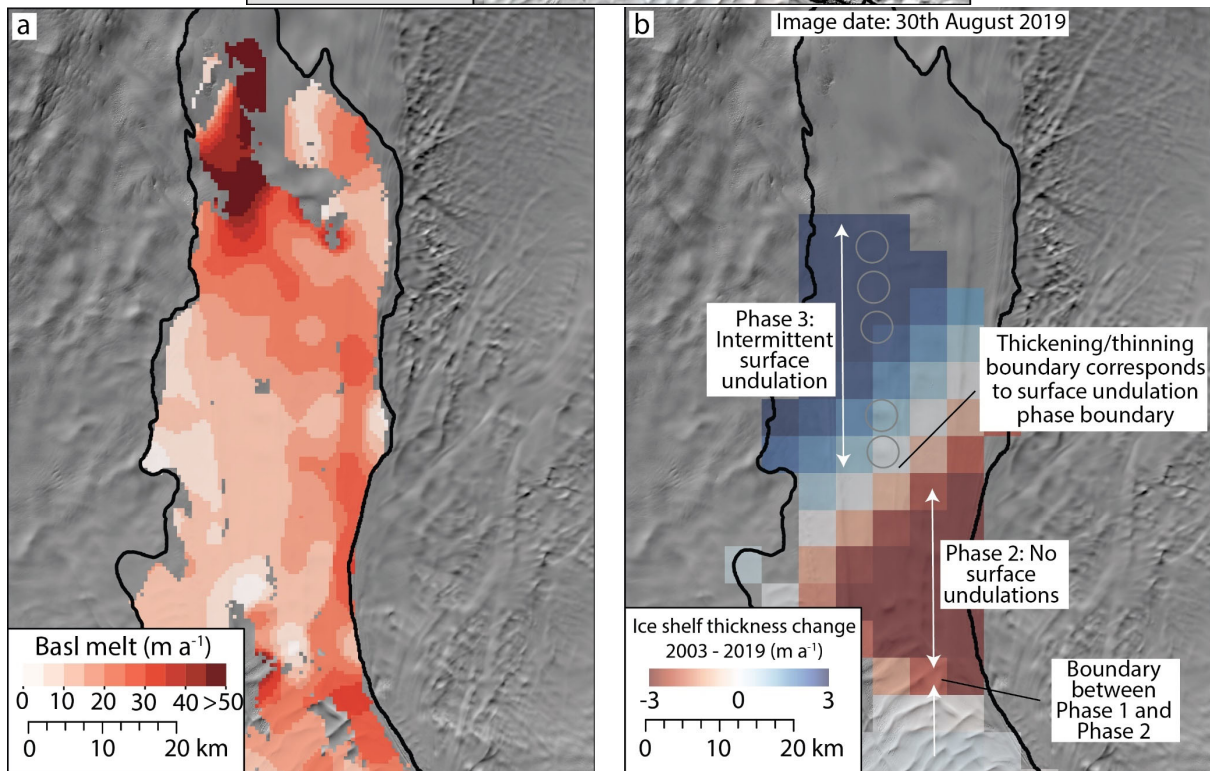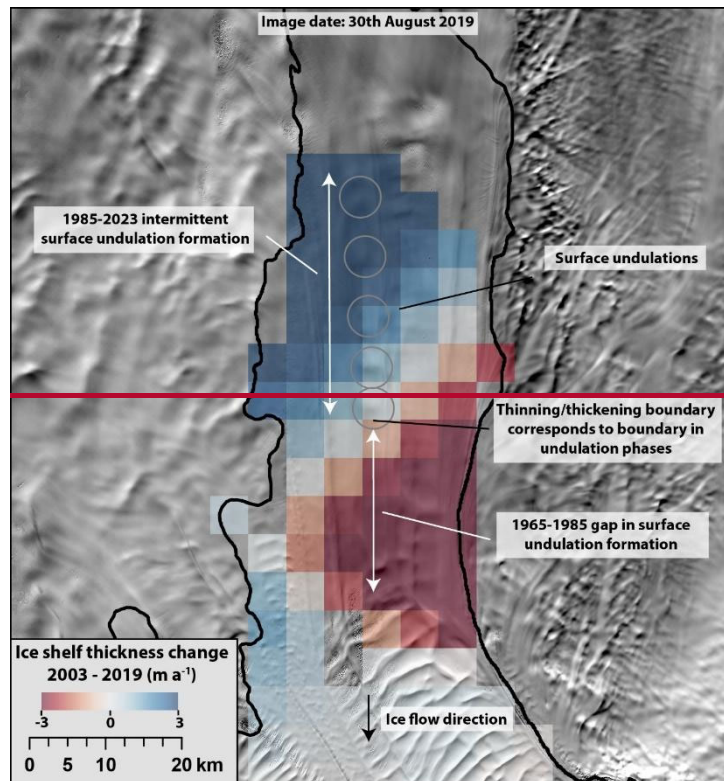
Figure 98: a) Basal—-melt rates averaged from 2010-2018 (Adusumilli et al., 2020). b) Ice-shelf thickness change between 2003 and 2019 (Smith et al., 2020) overlain on a Landsat-8 image from August 2019. The grey circles highlight visible surface undulations in the Landsat image from August 2019. Black line on both images is the MODIS 2009 grounding line (Haran, 2021; Scambos et al., 2007). Landsat images courtesy of U.S. Geological Survey.

4.54 Warm environmental conditions during the mid-20th century trigger mass loss?

568 We hypothesise that anomalously high ~~basal~~ basal-melt rates in the mid-20th century could
569 have ~~marked~~ acted as the trigger for the current mass loss of Totten Glacier. This could have
570 manifested via anomalously ~~anonymously~~ warm conditions causing the ice shelf to detach from
571 a pinning point. A candidate could be the partial detachment from the main ice rumple near the
572 grounding line, where the precise bed topography is still uncertain (Vaňková et al., 2023). At
573 the very least, the period of no surface-undulation formation in the mid-20th century likely
574 marked a period of unusually sustained higher basal-melt rates, with respect to conditions over
575 the past 100 years (Fig. 8~~7c~~c).

576 ~~The pattern of surface-undulation formation over the past 100 years also supports the notion of~~
577 ~~a long-term thinning of Totten Ice Shelf since the mid-20th century. Following the period of~~
578 ~~regular surface-undulation formation in the first half of the 20th century, surface undulations,~~
579 ~~despite some decadal variability, progressively become less frequent and visibly smaller in size~~
580 ~~(Fig. 7c). We interpret this as a long-term thinning of the ice shelf in response to increased melt~~
581 ~~rates, meaning increasingly more extreme cold anomalies are required for undulation formation.~~
582 ~~This is consistent with ship-based observations of ocean temperature that show a warming of~~
583 ~~CDW at the continental shelf adject to Totten Glacier between 1930-1990 and 2010-2018, in~~
584 ~~response to a wind-driven southward shift of the Antarctic Coastal Current (Herraiz-~~
585 ~~Borreguero and Naveira Garabato, 2022; Yamazaki et al., 2021). However,~~ Validating the
586 hypothesised period of anomalously warm conditions in the mid-20th century with reanalysis
587 or other sources of observational data is challenging. Outputs from ice-ocean models
588 reconstructing temporal variability in basal-melt rates back to the mid-20th century show
589 conflicting signals (Gwyther et al., 2018; Kusahara et al., 2024), and the reliability of key
590 climatic reanalysis input data throughout much of the early to mid-20th century is unknown.
591 There ~~is also~~ also remains ~~a poor understanding~~ insufficient resolution of the sub-ice-shelf
592 bathymetry that is crucial to simulating melt rates (Kusahara et al., 2024). ~~superimposed on~~
593 ~~this longer-term trend of CDW warming are the processes that modulate the delivery of mCDW~~
594 ~~onto the continental shelf and then towards ice-shelf cavities that are an important factor in the~~
595 ~~observed decadal variability in melt rates (Adusumilli et al., 2020; Roberts et al., 2018) and~~
596 ~~subsequent surface-undulation formation (Fig. 7c). In the case of Totten Glacier and Ice Shelf,~~
597 ~~several processes have been put forward to explain decadal variability in melt rates including~~
598 ~~variations in Antarctic Slope Current strength (Nakayama et al., 2021), intrinsic variability~~
599 ~~(Gwyther et al., 2018), zonal wind strength on the continental-shelf break (Greene et al., 2017)~~
600 ~~and coastal-polynya activity (Gwyther et al., 2014; Khazendar et al., 2013).~~

601 ~~Validating the hypothesised period of anonymously warm conditions in the mid-20th century~~
602 ~~with reanalysis data is challenging. Outputs from ice-ocean models reconstructing temporal~~
603 ~~variability in basal-melt rates back to the mid-20th century show conflicting signals (Gwyther~~
604 ~~et al., 2018; Kusahara et al., 2024), and the reliability of key climatic reanalysis input data~~
605 ~~throughout much of the early to mid-20th century is unknown. There is also a poor~~
606 ~~understanding of the sub-ice-shelf bathymetry that is crucial to simulating melt rates (Kusahara~~
607 ~~et al., 2024). However,~~ ~~M~~modern observations show synchronous ice-speed and ice-shelf
608 thickness anomalies throughout the 2000s at major outlet glaciers across the wider Wilkes Land
609 region (Miles et al., 2022). Therefore, any anomalously ~~anonymously~~ warm conditions in the
610 mid-20th century could have been felt regionally and not just at Totten Glacier. We observe the
611 collapse of a previously unreported ice shelf 50 km east of the ice front of Moscow University
612 Ice Shelf between 1963 and 1973 (Fig. 10~~9~~). The ice shelf is small (250 km^2) and did not

buttress any large glaciers, so its collapse is inconsequential for sea-level rise. The unnamed ice shelf was previously adjoined to Voyeykov Ice Shelf through a mixture of fast ice and melange. Voyeykov Ice Shelf periodically collapses and regrows in response to changes in fast ice conditions (Arthur et al., 2021), but at the unnamed ice shelf we observe no signs of regrowth in the fifty years following 50 years post its collapse (Fig. 10~~9~~). The final stages of ice-shelf collapse may be preceded by years or even decades of gradual weakening (Walker et al., 2024), meaning the collapse of this unnamed ice shelf at some point between 1963 and 1973 is consistent with relatively warm environmental conditions in the years or decades earlier and is symbolic of environmental change in the mid-20th Century.
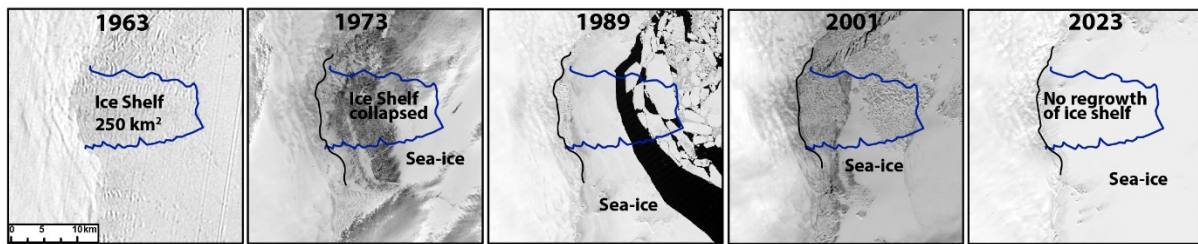
Figure 10~~9~~: A series of satellite images showing the disintegration of an un-named ice shelf between 1963 and 1973, which has not regrown to a comparable extent in the 50 years since. The blue line denotes the boundary of the ice shelf in 1963. The black line is the ice-front position in 2023. Satellite images are courtesy of the U.S. Geological Survey. See Figure 1a for location.

The century-long record of surface undulations implies that the ~30-year record of satellite altimetry is not long enough to capture the full extent of the amplitude and wavelength of decadal variability in basal-melt anomalies. Numerical-modelling experiments have shown that forcing Totten Glacier with variable basal-melt rates, at similar amplitudes to those inferred by ~30 years of satellite-altimetry observations, has a net effect of reducing ice discharge and delaying grounding-line retreat in comparison to constant forcing (McCormack et al., 2021). Therefore, evidence of prolonged periods of higher sustained melt rates in the ~~recent~~ mid-20th century ~~past~~ raises the possibility of similar episodes of accelerating retreat in the coming decades ~~accelerating retreat~~. Elsewhere, interpretations of surface features on ~~the~~West Antarctica's Venable ice Shelf have revealed intermittent local re-grounding on a pinning point since the 1930s (Locke et al., 2025), implying similar decadal variability in basal-melt rates. A greater understanding of the processes and the magnitude of decadal variability is vital to narrowing uncertainties in future sea-level projections from Antarctica (e.g. Hanna et al., 2024). It could be that ~~these~~ anomalous periods of warm oceanic conditions play a vital role in ~~kick starting~~triggering cycles of glacier retreat. Perhaps analogous to this ~~is~~ are Pine Island and Thwaites glaciers, where sediment records point to their retreat from ~~stabilizing~~ stabilising pinning points in the 1940s (Clark et al., 2024; Smith et al., 2017) in response to anomalously ~~anonymously~~ warm environmental conditions (Steig et al., 2012). The key difference here is that bedrock geometry at Pine Island Glacier was conducive for marine ice-sheet instability and a rapid retreat (Reed et al., 2024), whereas the present geometry at Totten Glacier is not favourable for a similar rapid retreat in the near future (Morlighem et al., 2020).

5. Conclusion

Overall, our results have shown that averaged decadal ice speed of Totten Ice Shelf has not accelerated over the past half-century. The combination of observations of inland thinning in the earliest satellite-altimetry records, grounding-line retreat between 1973 and 1989, and the absence of any long-term trends in snowfall, points towards the mass balance of Totten Glacier during this period ~~already being out of balance in the 1970s~~being similar to present. Therefore, the initial increase in ice discharge that placed Totten Glacier out of balance must have taken place before 1973. The near century-long record of surface-undulation formation highlights an anomalous ~20-year period in the mid-20th century that we interpret as sustained higher-than-average basal-melt rates causing much more limited interaction between a ~~prominent ice rumple~~bathymetric high point near the grounding line and the ice shelf. This interpretation is supported by satellite-altimetry observations that show waves of ice thickness variations travelling with ice flow that match the gap in surface-undulation formation. We ~~hypothesize~~ hypothesise that these anomalously ~~anonymously~~ warm conditions in the mid-20th century could have ~~marked the onset of the modern-day~~accelerated mass loss of Totten Glacier by ~~accelerating the detachment from a~~decoupling from a key pinning point, and/or marking a change in environmental conditions represented by more frequent and/or intense intrusions of mCDW onto the continental shelf. We also observe the collapse of a small neighbouring ice shelf during this period. Validating this proposed anomalously ~~anonymously~~ warm period is challenging because the drivers of interannual variability in melt rates at Totten Ice Shelf over the observational period are not fully understood. Perhaps more importantly, because surface undulations have been forming over the past ~30 years, our observations hint at warmer than present conditions in the recent past. Therefore, basal-melt rates calculated from short satellite-altimetry records that are often used as a baseline in numerical models to project into the future may not be capturing the full variability within the Totten glacier system.

Data availability: Landsat and ARGON imagery was provided free of charge by the U.S. Geological Survey Earth Resources Observation Science Center (https://earthexplorer.usgs.gov/, USGS, 2022). The MOA grounding line product is available at https://doi.org/10.7265/N5KP8037 (Haran, 2021). The ice shelf thickness change dataset from Smith et al. (2020) is available at http://hdl.handle.net/1773/45388 (last access: April 2022). The REMA DEM is available at https://doi.org/10.7910/DVN/X7NDNY (Howat et al., 2019). ICESat-2 data is available from https://nsidc.org/data/atl06/versions/6. The MEaSUREs Annual Antarctic Ice Velocity Maps are available at https://doi.org/10.5067/9T4EPQXTJYW9. Bathymetry and in situ basal-melt timeseries are available at https://doi.org/10.6084/m9.figshare.21824580 (Vaňková et al., 2023). Corrected Landsat

imagery of Antarctic ice shelves from 1973 and 1989 is available at https://doi.org/10.7488/ds/3810 (Miles and Bingham, 2023). BedMachine version 3 is available at https://doi.org/10.5067/FPSU0V1MWUB6 (Morlighem, 2022). MEaSUREs ITS_LIVE Antarctic Grounded Ice Sheet Elevation Change is available at https://doi.org/10.5067/L3LSVDZS15ZV (Nilsson et al., 2025) Corrected Argon ARGON imagery was provided by Ron Li. The decadal ice speed tracking vectors and grounding line mapping from this study are available at https://doi.org/10.7488/ds/7853.

Acknowledgements: Bertie W. J. Miles was supported by a Leverhulme Early Career Fellowship (ECF-2021-484). Tian Li is funded by the European Union's Horizon 2020 research and innovation programme through the project Arctic PASSION (grant number: 101003472) and the Leverhulme Early Career Fellowship (ECF-2024-157). Robert G. Bingham acknowledges funding from NERC (NE/S006613/1).

Author Contribution: B.M led the design of the study with input from T.L and R.G.B. T.L produced Ffigure 7da and carried out the ICESat-2 analysis. B.M led the manuscript writing with input from T.L and R.G.B

Competing interests: The authors declare that they have no conflict of interest.

References

Adusumilli, S., Fricker, H. A., Medley, B., Padman, L., and Siegfried, M. R.: Interannual variations in meltwater input to the Southern Ocean from Antarctic ice shelves, Nature Geoscience, 13, 616-620, 2020.

Aitken, A. R. A., Roberts, J. L., Ommen, T. D. v., Young, D. A., Golledge, N. R., Greenbaum, J. S., Blankenship, D. D., and Siegert, M. J.: Repeated large-scale retreat and advance of Totten Glacier indicated by inland bed erosion, Nature, 533, 385-389, 2016.

Arthur, J. F., Stokes, C. R., Jamieson, S. S. R., Miles, B. W. J., Carr, J. R., and Leeson, A. A.: The triggers of the disaggregation of Voyeykov Ice Shelf (2007), Wilkes Land, East Antarctica, and its subsequent evolution, Journal of Glaciology, 67, 933-951, 2021.

Baumhoer, C. A., Dietz, A. J., Kneisel, C., Paeth, H., and Kuenzer, C.: Environmental drivers of circum-Antarctic glacier and ice shelf front retreat over the last two decades, The Cryosphere, 15, 2357-2381, 2021.

Bindschadler, R., Vaughan, D. G., and Vornberger, P.: Variability of basal melt beneath the Pine Island Glacier ice shelf, West Antarctica, Journal of Glaciology, 57, 581-595, 2011.

Brancato, V., Rignot, E., Milillo, P., Morlighem, M., Mouginot, J., An, L., Scheuchl, B., Jeong, S., Rizzoli, P., Bueso Bello, J. L., and Prats-Iraola, P.: Grounding Line Retreat of Denman Glacier, East Antarctica, Measured With COSMO-SkyMed Radar Interferometry Data, Geophysical Research Letters, 47, e2019GL086291, 2020.

Brunt, K. M., Fricker, H. A., and Padman, L.: Analysis of ice plains of the Filchner–Ronne Ice Shelf, Antarctica, using ICESat laser altimetry, Journal of Glaciology, 57, 965-975, 2011.

Christie, F. D. W., Bingham, R. G., Gourmelen, N., Tett, S. F. B., and Muto, A.: Four-decade record of pervasive grounding line retreat along the Bellingshausen margin of West Antarctica, Geophysical Research Letters, 43, 5741-5749, 2016.

Clark, R. W., Wellner, J. S., Hillenbrand, C.-D., Totten, R. L., Smith, J. A., Miller, L. E., Larter, R. D., Hogan, K. A., Graham, A. G. C., Nitsche, F. O., Lehrmann, A. A., Lepp, A. P., Kirkham, J. D., Fitzgerald, V. T., Garcia-Barrera, G., Ehrmann, W., and Wacker, L.: Synchronous retreat of Thwaites and Pine Island glaciers in response to external forcings in the presatellite era, Proceedings of the National Academy of Sciences, 121, e2211711120, 2024.

Cook, C. P., Hill, D. J., van de Flierdt, T., Williams, T., Hemming, S. R., Dolan, A. M., Pierce, E. L., Escutia, C., Harwood, D., Cortese, G., and Gonzales, J. J.: Sea surface temperature control on the distribution of far-traveled Southern Ocean ice-rafted detritus during the Pliocene, Paleoceanography, 29, 533-548, 2014.

Davison, B. J., Hogg, A. E., Slater, T., and Rigby, R.: Antarctic Ice Sheet grounding line discharge from 1996 through 2023, Earth Syst. Sci. Data Discuss., 2023, 1-35, 2023.

De Rydt, J., Gudmundsson, G. H., Corr, H. F. J., and Christoffersen, P.: Surface undulations of Antarctic ice streams tightly controlled by bedrock topography, The Cryosphere, 7, 407-417, 2013.

Floricioiu, D. K., L.; Chowdhury, T.A.; Bässler, M: ESA Antarctic Ice Sheet Climate Change Initiative (Antarctic_Ice_Sheet_cci): Grounding line location for key glaciers, Antarctica, 1994-2020, v2.0. NERC EDS Centre for Environmental Data Analysis, 2021.

Fricker, H. A., Coleman, R., Padman, L., Scambos, T. A., Bohlander, J., and Brunt, K. M.: Mapping the grounding zone of the Amery Ice Shelf, East Antarctica using InSAR, MODIS and ICESat, Antarctic Science, 21, 515-532, 2009.

Greenbaum, J. S., Blankenship, D. D., Young, D. A., Richter, T. G., Roberts, J. L., Aitken, A. R. A., Legresy, B., Schroeder, D. M., Warner, R. C., van Ommen, T. D., and Siegert, M. J.: Ocean access to a cavity beneath Totten Glacier in East Antarctica, Nature Geoscience, 8, 294-298, 2015.

Greene, C. A., Blankenship, D. D., Gwyther, D. E., Silvano, A., and Van Wijk, E.: Wind causes Totten Ice Shelf melt and acceleration, Science Advances, 3, e1701681-e1701681, 2017.

Gudmundsson, G. H.: Transmission of basal variability to a glacier surface, Journal of Geophysical Research: Solid Earth, 108, 2003.

Gwyther, D. E., Galton-Fenzi, B. K., Hunter, J. R., and Roberts, J. L.: Simulated melt rates for the Totten and Dalton ice shelves, Ocean Sci., 10, 267-279, 2014.

Gwyther, D. E., O'Kane, T. J., Galton-Fenzi, B. K., Monselesan, D. P., and Greenbaum, J. S.: Intrinsic processes drive variability in basal melting of the Totten Glacier Ice Shelf, Nature Communications, 9, 3141, 2018.

Hanna, E., Topál, D., Box, J. E., Buzzard, S., Christie, F. D. W., Hvidberg, C., Morlighem, M., De Santis, L., Silvano, A., Colleoni, F., Sasgen, I., Banwell, A. F., van den Broeke, M. R., DeConto, R., De Rydt, J., Goelzer, H., Gossart, A., Gudmundsson, G. H., Lindbäck, K., Miles, B., Mottram, R., Pattyn, F., Reese, R., Rignot, E., Srivastava, A., Sun, S., Toller, J.,

776   Tuckett, P. A., and Ultee, L.: Short- and long-term variability of the Antarctic and
777   Greenland ice sheets, Nature Reviews Earth & Environment, 5, 193-210, 2024.

778 Haran, T., Bohlander, J., Scambos, T., Painter, T. & Fahnestock, M.: MODIS Mosaic of
779   Antarctica 2008-2009 (MOA2009) Image Map. (NSIDC-0593, Version 2). Boulder, C. U.
780   (Ed.), NASA National Snow and Ice Data Center Distributed Active Archive Center, 2021.

781 Herraiz-Borreguero, L. and Naveira Garabato, A. C.: Poleward shift of Circumpolar Deep
782   Water threatens the East Antarctic Ice Sheet, Nature Climate Change, 12, 728-734, 2022.

783 Hirano, D., Tamura, T., Kusahara, K., Fujii, M., Yamazaki, K., Nakayama, Y., Ono, K., Itaki,
784   T., Aoyama, Y., Simizu, D., Mizobata, K., Ohshima, K. I., Nogi, Y., Rintoul, S. R., van
785   Wijk, E., Greenbaum, J. S., Blankenship, D. D., Saito, K., and Aoki, S.: On-shelf
786   circulation of warm water toward the Totten Ice Shelf in East Antarctica, Nature
787   Communications, 14, 4955, 2023.

788 Howat, I. M., Porter, C., Smith, B. E., Noh, M. J., and Morin, P.: The Reference Elevation
789   Model of Antarctica, The Cryosphere, 13, 665-674, 2019.

790 Jong, L. M., Plummer, C. T., Roberts, J. L., Moy, A. D., Curran, M. A. J., Vance, T. R., Pedro,
791   J. B., Long, C. A., Nation, M., Mayewski, P. A., and van Ommen, T. D.: 2000 years of
792   annual ice core data from Law Dome, East Antarctica, Earth Syst. Sci. Data, 14, 3313-
793   3328, 2022.

794 Jordan, J. R., Miles, B. W. J., Gudmundsson, G. H., Jamieson, S. S. R., Jenkins, A., and Stokes,
795   C. R.: Increased warm water intrusions could cause mass loss in East Antarctica during
796   the next 200 years, Nature Communications, 14, 1825, 2023.

797 Khazendar, A., Schodlok, M. P., Fenty, I., Ligtenberg, S. R. M., Rignot, E., and van den Broeke,
798   M. R.: Observed thinning of Totten Glacier is linked to coastal polynya variability, Nature
799   Communications, 4, 2857, 2013.

800 Kim, B.-H., Seo, K.-W., Lee, C.-K., Kim, J.-S., Lee, W. S., Jin, E. K., and van den Broeke, M.:
801   Partitioning the drivers of Antarctic glacier mass balance (2003–2020) using satellite
802   observations and a regional climate model, Proceedings of the National Academy of
803   Sciences, 121, e2322622121, 2024.

804 Kim, S. H., Kim, D.-j., and Kim, H.-C.: Progressive Degradation of an Ice Rumple in the
805   Thwaites Ice Shelf, Antarctica, as Observed from High-Resolution Digital Elevation
806   Models, Remote Sensing, 10, 1236, 2018.

807 Kusahara, K., Hirano, D., Fujii, M., Fraser, A. D., Tamura, T., Mizobata, K., Williams, G. D.,
808   and Aoki, S.: Modeling seasonal-to-decadal ocean–cryosphere interactions along the
809   Sabrina Coast, East Antarctica, The Cryosphere, 18, 43-73, 2024.

810 Lee, C.-K., Seo, K.-W., Han, S.-C., Yu, J., and Scambos, T. A.: Ice velocity mapping of Ross
811   Ice Shelf, Antarctica by matching surface undulations measured by ICESat laser altimetry,
812   Remote Sensing of Environment, 124, 251-258, 2012.

813 Li, R., Cheng, Y., Chang, T., Gwyther, D. E., Forbes, M., An, L., Xia, M., Yuan, X., Qiao, G.,
814   Tong, X., and Ye, W.: Satellite record reveals 1960s acceleration of Totten Ice Shelf in
815   East Antarctica, Nature Communications, 14, 4061, 2023a.

816 Li, R., Cheng, Y., Cui, H., Xia, M., Yuan, X., Li, Z., Luo, S., and Qiao, G.: Overestimation and
817   adjustment of Antarctic ice flow velocity fields reconstructed from historical satellite
818   imagery, The Cryosphere, 16, 737-760, 2022.

Li, T., Dawson, G. J., Chuter, S. J., and Bamber, J. L.: Grounding line retreat and tide-modulated ocean channels at Moscow University and Totten Glacier ice shelves, East Antarctica, The Cryosphere, 17, 1003-1022, 2023b.

Li, X., Rignot, E., Morlighem, M., Mouginot, J., and Scheuchl, B.: Grounding line retreat of Totten Glacier, East Antarctica, 1996 to 2013. In: Geophysical Research Letters, Blackwell Publishing Ltd, 2015.

Locke, C. D., Tinto, K. J., Porter, D. F., & Constantino, R. R. (2025). Novel record of intermittent grounding of the Venable Ice Shelf since 1935 from Operation IceBridge airborne-gravity-derived bathymetry and Landsat imagery. Geophysical Research Letters, 52, e2024GL114071. https://doi.org/10.1029/2024GL114071

Luckman, A., Jansen, D., Kulessa, B., King, E. C., Sammonds, P., and Benn, D. I.: Basal crevasses in Larsen C Ice Shelf and implications for their global abundance, The Cryosphere, 6, 113–123, https://doi.org/10.5194/tc-6-113-2012, 2012.

Martínez-Botí, M. A., Foster, G. L., Chalk, T. B., Rohling, E. J., Sexton, P. F., Lunt, D. J., Pancost, R. D., Badger, M. P. S., and Schmidt, D. N.: Plio-Pleistocene climate sensitivity evaluated using high-resolution CO_2 records, Nature, 518, 49-54, 2015.

McCormack, F. S., Roberts, J. L., Gwyther, D. E., Morlighem, M., Pelle, T., and Galton-Fenzi, B. K.: The Impact of Variable Ocean Temperatures on Totten Glacier Stability and Discharge, Geophysical Research Letters, 48, e2020GL091790, 2021.

McGrath, D., Steffen, K., Scambos, T., Rajaram, H., Casassa, G., and Rodriguez Lagos, J. L.: Basal crevasses and associated surface crevassing on the Larsen C ice shelf, Antarctica, and their role in ice-shelf instability, Ann. Glaciol., 53, 10–18, https://doi.org/10.3189/2012AoG60A005, 2012

Miles, B. and Bingham, R.: Landsat mosaics of Antarctic Ice Shelves from 1973 and 1989, 1973-1989 [dataset], University of Edinburgh. School of Geosciences., doi: https://doi.org/10.7488/ds/3810, 2023. 2023.

Miles, B. W. J. and Bingham, R. G.: Progressive unanchoring of Antarctic ice shelves since 1973, Nature, 626, 785-791, 2024.

Miles, B. W. J., Stokes, C. R., and Jamieson, S. S. R.: Pan-ice-sheet glacier terminus change in East Antarctica reveals sensitivity of Wilkes Land to sea-ice changes, Science advances, 2, e1501350-e1501350, 2016.

Miles, B. W. J., Stokes, C. R., Jamieson, S. S. R., Jordan, J. R., Gudmundsson, G. H., and Jenkins, A.: High spatial and temporal variability in Antarctic ice discharge linked to ice shelf buttressing and bed geometry, Scientific Reports, 12, 10968, 2022.

Mohajerani, Y., Velicogna, I., and Rignot, E.: Mass Loss of Totten and Moscow University Glaciers, East Antarctica, Using Regionally Optimized GRACE Mascons, Geophysical Research Letters, 45, 7010-7018, 2018.

Morlighem, M., Rignot, E., Binder, T., Blankenship, D., Drews, R., Eagles, G., Eisen, O., Ferraccioli, F., Forsberg, R., Fretwell, P., Goel, V., Greenbaum, J. S., Gudmundsson, H., Guo, J., Helm, V., Hofstede, C., Howat, I., Humbert, A., Jokat, W., Karlsson, N. B., Lee, W. S., Matsuoka, K., Millan, R., Mouginot, J., Paden, J., Pattyn, F., Roberts, J., Rosier, S., Ruppel, A., Seroussi, H., Smith, E. C., Steinhage, D., Sun, B., Broeke, M. R. v. d., Ommen, T. D. v., Wessem, M. v., and Young, D. A.: Deep glacial troughs and stabilizing ridges unveiled beneath the margins of the Antarctic ice sheet, Nature Geoscience, 13, 132-137, 2020.

Morlighem, M. (2022). MEaSUREs BedMachine Antarctica. (NSIDC-0756, Version 3). [Data Set]. Boulder, Colorado USA. NASA National Snow and Ice Data Center Distributed Active Archive Center. https://doi.org/10.5067/FPSU0V1MWUB6.

Mouginot, J., Rignot, E., Scheuchl, B. & Millan, R.. 2017. Comprehensive Annual Ice Sheet Velocity Mapping Using Landsat-8, Sentinel-1, and RADARSAT-2 Data. Remote Sensing. 9. DOI: 10.3390/rs9040364.

Nakayama, Y., Greene, C. A., Paolo, F. S., Mensah, V., Zhang, H., Kashiwase, H., Simizu, D., Greenbaum, J. S., Blankenship, D. D., Abe-Ouchi, A., and Aoki, S.: Antarctic Slope Current Modulates Ocean Heat Intrusions Towards Totten Glacier, Geophysical Research Letters, 48, e2021GL094149, 2021.

Nakayama, Y., Wongpan, P., Greenbaum, J. S., Yamazaki, K., Noguchi, T., Simizu, D., Kashiwase, H., Blankenship, D. D., Tamura, T., and Aoki, S.: Helicopter-Based Ocean Observations Capture Broad Ocean Heat Intrusions Toward the Totten Ice Shelf, Geophysical Research Letters, 50, e2022GL097864, 2023.

Nilsson, J., Gardner, A. S., and Paolo, F. S.: Elevation change of the Antarctic Ice Sheet: 1985 to 2020, Earth Syst. Sci. Data, 14, 3573-3598, 2022.

Padman, L., Fricker, H. A., Coleman, R., Howard, S., and Erofeeva, L.: A new tide model for the Antarctic ice shelves and seas, Annals of Glaciology, 34, 247-254, 2002.

Paolo, F. S., Fricker, H. A., Padman, L., and Fs Paolo, H. A. F. L. P.: Volume loss from Antarctic ice shelves is accelerating, Science, 348, 327-331, 2015.

Pelle, T., Morlighem, M., Nakayama, Y., and Seroussi, H.: Widespread Grounding Line Retreat of Totten Glacier, East Antarctica, Over the 21st Century, Geophysical Research Letters, 48, e2021GL093213, 2021.

Picton, H. J., Stokes, C. R., Jamieson, S. S. R., Floricioiu, D., and Krieger, L.: Extensive and anomalous grounding line retreat at Vanderford Glacier, Vincennes Bay, Wilkes Land, East Antarctica, The Cryosphere, 17, 3593-3616, 2023.

Reed, B., Green, J. A. M., Jenkins, A., and Gudmundsson, G. H.: Recent irreversible retreat phase of Pine Island Glacier, Nature Climate Change, 14, 75-81, 2024.

Ribeiro, N., Herraiz-Borreguero, L., Rintoul, S. R., McMahon, C. R., Hindell, M., Harcourt, R., and Williams, G.: Warm Modified Circumpolar Deep Water Intrusions Drive Ice Shelf Melt and Inhibit Dense Shelf Water Formation in Vincennes Bay, East Antarctica, Journal of Geophysical Research: Oceans, 126, e2020JC016998, 2021.

Rignot, E., Mouginot, J., and Scheuchl, B.: Ice flow of the antarctic ice sheet, Science, 333, 1427-1430, 2011.

Rignot, E., Mouginot, J., Scheuchl, B., Van Den Broeke, M., Van Wessem, M. J., and Morlighem, M.: Four decades of Antarctic ice sheet mass balance from 1979–2017, Proceedings of the National Academy of Sciences of the United States of America, 116, 1095-1103, 2019.

Rintoul, S. R., Silvano, A., Pena-Molino, B., Van Wijk, E., Rosenberg, M., Greenbaum, J. S., and Blankenship, D. D.: Ocean heat drives rapid basal melt of the totten ice shelf, Science Advances, 2, 2016.

Roberts, J., Galton-Fenzi Benjamin, K., Paolo Fernando, S., Donnelly, C., Gwyther David, E., Padman, L., Young, D., Warner, R., Greenbaum, J., Fricker Helen, A., Payne Antony, J., Cornford, S., Le Brocq, A., van Ommen, T., Blankenship, D., and Siegert Martin, J.: Ocean

forced variability of Totten Glacier mass loss, Geological Society, London, Special Publications, 461, 175-186, 2018.

Roberts, J., Plummer, C., Vance, T., van Ommen, T., Moy, A., Poynter, S., Treverrow, A., Curran, M., and George, S.: A 2000-year annual record of snow accumulation rates for Law Dome, East Antarctica, Clim. Past, 11, 697-707, 2015.

Scambos, T. A., Haran, T. M., Fahnestock, M. A., Painter, T. H., and Bohlander, J.: MODIS-based Mosaic of Antarctica (MOA) data sets: Continent-wide surface morphology and snow grain size, Remote Sensing of Environment, 111, 242-257, 2007.

Schröder, L., Horwath, M., Dietrich, R., Helm, V., van den Broeke, M. R., and Ligtenberg, S. R. M.: Four decades of Antarctic surface elevation changes from multi-mission satellite altimetry, The Cryosphere, 13, 427-449, 2019.

Silvano, A., Rintoul, S. R., Peña-Molino, B., and Williams, G. D.: Distribution of water masses and meltwater on the continental shelf near the Totten and Moscow University ice shelves, Journal of Geophysical Research: Oceans, 122, 2050-2068, 2017.

Smith, B., Fricker, H. A., Gardner, A. S., Medley, B., Nilsson, J., Paolo Nicholas Holschuh, F. S., Adusumilli, S., Brunt, K., Csatho, B., Harbeck, K., Markus, T., Neumann, T., Siegfried, M. R., and Jay Zwally, H.: Pervasive ice sheet mass loss reflects competing ocean and atmosphere processes, Science, 368, 1239-1242, 2020.

Smith, B., Fricker, H. A., Holschuh, N., Gardner, A. S., Adusumilli, S., Brunt, K. M., Csatho, B., Harbeck, K., Huth, A., Neumann, T., Nilsson, J., and Siegfried, M. R.: Land ice height-retrieval algorithm for NASA's ICESat-2 photon-counting laser altimeter, Remote Sensing of Environment, 233, 111352, 2019.

Smith, J. A., Andersen, T. J., Shortt, M., Gaffney, A. M., Truffer, M., Stanton, T. P., Bindschadler, R., Dutrieux, P., Jenkins, A., Hillenbrand, C. D., Ehrmann, W., Corr, H. F. J., Farley, N., Crowhurst, S., and Vaughan, D. G.: Sub-ice-shelf sediments record history of twentieth-century retreat of Pine Island Glacier, Nature, 541, 77-80, 2017.

Steig, E. J., Ding, Q., Battisti, D. S., and Jenkins, A.: Tropical forcing of circumpolar deep water inflow and outlet glacier thinning in the amundsen sea embayment, west antarctica, Annals of Glaciology, 53, 19-28, 2012.

Stokes, C. R., Abram, N. J., Bentley, M. J., Edwards, T. L., England, M. H., Foppert, A., Jamieson, S. S. R., Jones, R. S., King, M. A., Lenaerts, J. T. M., Medley, B., Miles, B. W. J., Paxman, G. J. G., Ritz, C., van de Flierdt, T., and Whitehouse, P. L.: Response of the East Antarctic Ice Sheet to past and future climate change, Nature, 608, 275-286, 2022.

van Dalum, C. T., van de Berg, W. J., Gadde, S. N., van Tiggelen, M., van der Drift, T., van Meijgaard, E., van Ulft, L. H., and van den Broeke, M. R.: First results of the polar regional climate model RACMO2.4, The Cryosphere, 18, 4065–4088, https://doi.org/10.5194/tc-18-4065-2024, 2024.

van Wijk, E. M., Rintoul, S. R., Wallace, L. O., Ribeiro, N., and Herraiz-Borreguero, L.: Vulnerability of Denman Glacier to Ocean Heat Flux Revealed by Profiling Float Observations, Geophysical Research Letters, 49, e2022GL100460, 2022.

Vaňková, I., Winberry, J. P., Cook, S., Nicholls, K. W., Greene, C. A., and Galton-Fenzi, B. K.: High Spatial Melt Rate Variability Near the Totten Glacier Grounding Zone Explained by New Bathymetry Inversion, Geophysical Research Letters, 50, e2023GL102960, 2023.

951 Walker, C. C., Millstein, J. D., Miles, B. W. J., Cook, S., Fraser, A. D., Colliander, A., Misra,
952   S., Trusel, L. D., Adusumilli, S., Roberts, C., and Fricker, H. A.: Multi-decadal collapse
953   of East Antarctica's Conger–Glenzer Ice Shelf, Nature Geoscience, doi: 10.1038/s41561-
954   024-01582-3, 2024. 2024.

955 Yamazaki, K., Aoki, S., Katsumata, K., Hirano, D., and Nakayama, Y.: Multidecadal poleward
956   shift of the southern boundary of the Antarctic Circumpolar Current off East Antarctica,
957   Science Advances, 7, eabf8755, 2021.

958 Ye, W., Qiao, G., Kong, F., Ma, X., Tong, X., and Li, R.: Improved Geometric Modeling of
959   1960s KH-5 ARGON Satellite Images for Regional Antarctica Applications,
960   Photogrammetric Engineering & Remote Sensing, 83, 477-491, 2017.

961